6 Derivatives of the radiation field and their application to the solution of inverse problems

V. V. Rozanov, A. V. Rozanov, A. A. Kokhanovsky

6.1 Introduction

Spectral distribution of the solar radiation traveling through the Earth's atmosphere contain an important information about numerous atmospheric and surface parameters. This information can be gained from the measured spectra employing so-called inverse theory and the problem to be solved thereby is usually referred to as the inverse problem. The first step to be done in the solution of any inverse problem is to formulate a model usually referred to as the forward model which will allow us to simulate the measured quantity assuming all relevant atmospheric and surface parameters to be known. Generally, in the case of the scattered, reflected, or transmitted solar radiance measured in the ultraviolet, visible, or near-infrared spectral range by means of satellite, airborne, or ground-based instruments, the corresponding forward model is nonlinear, i.e., there is no linear relationship between measured values of intensity and atmospheric parameters. However, the theoretical basis of the inverse problem solution is well investigated in the case of linear inverse problems only [19]. Thus, to make use of the existing numerical methods the forward model has to be linearized, i.e., a linear relationship between intensity of radiation and the atmospheric parameters has to be obtained. This can formally be done considering the intensity as a function or functional of the corresponding parameters and expanding it in the Taylor series with respect to the variations of the desired parameters. Then, in the linear approximation the partial or the variational derivatives of the intensity, usually referred to as the weighting functions (WFs), provide a linear relationship between the variation of the intensity and variations of parameters. Unfortunately, analytical expressions for the weighting functions can be derived in a few simple cases only whereas numerical calculations employing their mathematical definition in most practical situations are very computational-time-expensive.

In the previous issue of *Light Scattering Reviews* [24] we have presented a general approach to derive partial and variational derivatives based on the joint solution of the direct radiative transfer equation and the adjoint radiative transfer equation. Employing this approach we have derived the general expressions

for the partial and variational derivatives of the Stokes vector with respect to the main optical parameters such as the extinction coefficient and the single scattering albedo. However, most optical parameters depend not only on the atmospheric parameters (e.g., on concentrations of absorbing gases, pressure, temperature, aerosol and cloud particles number density) but also on the wavelength. Therefore, in multispectral inverse problems these are the atmospheric parameters which are commonly used as quantities to be retrieved rather than the optical parameters. For this reason we will derive here analytical expressions for WFs for the different atmospheric parameters which can be directly used to solve practical inverse problems. In particular, we will obtain WFs for the aerosol particles number density, for the atmospheric pressure and temperature, for the liquid water content and the effective radius of cloud droplets, as well as for geometrical cloud parameters such as cloud top height and geometrical cloud thickness. Furthermore, we will demonstrate that WFs for all considered atmospheric parameters can be obtained as a linear combination of WFs for main optical parameters.

Taking into account that for the solution of most inverse problems the scalar form of the radiative transfer equation is sufficient, we can simplify our treatment considering only variations of the intensity of radiation and neglecting other components of the Stokes vector, i.e., polarization effects. All expressions for WFs obtained here for the scalar case are implemented in the software package SCIATRAN 2.0 [22] and its successor version SCIATRAN 2.1 (see www.iup.uni-bremen.de/sciatran for further information). All numerical examples demonstrated throughout this chapter were completed employing the software package SCIATRAN 2.1.

The layout of the chapter is as follows. In section 6.2 we consider a relationship between the partial and variational derivatives of the intensity of radiation and the weighting functions. Section 6.3 gives the review the basics of the direct and adjoint radiative transfer equations which are used in the following sections for the derivation of WFs. In section 6.4 we derive general expressions for WFs. Section 6.5 presents expressions for WFs of the absorption and scattering coefficients. In section 6.6 we extend the obtained expressions to the case of a mixture of scattering and absorbing components. Numerical examples of WFs for the aerosol and cloud scattering coefficients are shown in section 6.7. In section 6.8 we derive WFs for the pressure and temperature and show some numerical examples in the ultraviolet and near infrared spectral ranges. Section 6.9 is aimed to the derivation of WFs for cloud parameters such as particle number density, liquid water content, and effective radius of water droplets or ice crystals. Some illustrations of these WFs are presented subsequently in section 6.10. In section 6.11 we introduce a modification for the weighting functions for the effective radius of water droples or ice crystals making them more suitable for the solution of the corresponding inverse problems. WFs for the geometrical cloud parameters such as cloud top and bottom height are presented in section 6.12. The derivation of WFs for main optical parameters such as the extinction coefficient and the single scattering albedo is presented in the Appendix.

6.2 Derivatives of the intensity and weighting functions

The intensity of the radiation field in a vertically inhomogeneous medium depends not only on the optical depth and the viewing direction but also on the vertical distribution of such parameters as, for example, the extinction coefficient and the single scattering albedo. This set of parameters depending on a vertical coordinate will be referred to as parameter-functions. In the case of the reflecting and emitting underlying surface the intensity depends also on the surface albedo, surface emissivity, etc. which will be referred to as scalar parameters. From the mathematical point of view the intensity can be considered as a functional of parameter-functions and a function of scalar parameters. A linear relationship between variations of these parameters and the variation of the intensity can be obtained employing the Taylor series expansion of the intensity. Restricting ourselves at this point with one parameter-function and one scalar parameter only which will be denoted as $p(\tau)$ and c, respectively, we have in the linear approximation:

$$I'(\tau,\Omega) = I(\tau,\Omega) + \frac{\partial I(\tau,\Omega)}{\partial c}\,\Delta c + \int_0^{\tau_0} \frac{\delta I(\tau,\Omega)}{\delta p(\tau')}\,\delta p(\tau')\,\mathrm{d}\tau' \,. \tag{6.1}$$

Here, $\tau \in [0,\tau_0]$ is the optical depth, τ_0 is the optical thickness of the medium, $\Omega := \{\mu,\phi\}$ describes the set of variables $\mu \in [-1,1]$ and $\phi \in [0,2\pi]$, μ and ϕ are the cosine of the polar angle and the azimuthal angle, respectively, the perturbed intensity, $I'(\tau,\Omega)$, corresponds to perturbed parameters $c' = c + \Delta c$ and $p'(\tau) = p(\tau) + \delta p(\tau)$,

$$\frac{\partial I(\tau,\Omega)}{\partial c} = \lim_{\Delta c \to 0} \frac{I(\tau,\Omega;p(\tau),c') - I(\tau,\Omega;p(\tau),c)}{\Delta c} \tag{6.2}$$

is the partial derivative of the intensity with respect to the scalar parameter c and

$$\frac{\delta I(\tau,\Omega)}{\delta p(\tau')} = \lim_{\Delta\tau' \to 0} \frac{I(\tau,\Omega;p'(\tau),c) - I(\tau,\Omega;p(\tau),c)}{\int_{(\Delta\tau')} \delta p(x)\,\mathrm{d}x} \tag{6.3}$$

is the variational derivative of the intensity with respect to the parameter-function $p(\tau)$ at the optical depth $\tau' \in [0,\tau_0]$. The integration of the perturbation in the denominator of this expression is carried out over a small range $\Delta\tau'$ around the point τ' where $\delta p(x)$ is non-zero. A complete discussion of functionals and variational derivatives is presented among others by Volterra [33]. The partial derivative at a given optical depth τ and viewing direction Ω given by (6.2) will be considered as a function of the wavelength, whereas the variational derivative given by (6.3) as a function of the vertical coordinate τ' and the wavelength. The explicit notation of the dependence of all relevant functions on the wavelength will be omitted.

Introducing the variation of the intensity as

$$\delta I(\tau,\Omega) = I'(\tau,\Omega) - I(\tau,\Omega)\,, \tag{6.4}$$

we rewrite (6.1) in the following form:

$$\delta I(\tau,\Omega) = \mathcal{V}_c(\tau,\Omega)\Delta c + \int_0^{\tau_0} \mathcal{V}_p(\tau';\tau,\Omega)\delta p(\tau')\,\mathrm{d}\tau'\,, \tag{6.5}$$

where the variational and partial derivatives of the intensity are denoted as $\mathcal{V}_p(\tau';\tau,\Omega)$ and $\mathcal{V}_c(\tau,\Omega)$, respectively.

Equation (6.5) provides a linear relationship between variations of the atmospheric and surface parameters and the variation of the intensity at a given optical depth τ and viewing direction Ω. Functions $\mathcal{V}_p(\tau';\tau,\Omega)$ and $\mathcal{V}_c(\tau,\Omega)$ describe the contribution of the variation of a certain parameter to the variation of the intensity. These functions which are usually referred to as the weighting functions (WFs) can be defined for both absolute and relative variations of parameters. Introducing the relative variation of a scalar parameter c as $v_c = \Delta c/c$ and the relative variation of a parameter-function $p(\tau)$ as $v_p(\tau) = \delta p(\tau)/p(\tau)$, Eq. (6.5) can be rewritten as follows:

$$\delta I(\tau,\Omega) = \mathcal{W}_c(\tau,\Omega)v_c + \int_0^{\tau_0} \mathcal{W}_p(\tau';\tau,\Omega)v_p(\tau')\,\mathrm{d}\tau'\,. \tag{6.6}$$

The relationship between weighting functions for the relative and absolute variations of parameters is obvious:

$$\mathcal{W}_c(\tau,\Omega) = c\mathcal{V}_c(\tau,\Omega)\,,\quad \mathcal{W}_p(\tau';\tau,\Omega) = p(\tau')\mathcal{V}_p(\tau';\tau,\Omega)\,. \tag{6.7}$$

The obtained linear relationship between the variation of the intensity and variations of parameters can be directly used to solve various inverse problems. To demonstrate this let us consider the simplest case of one scalar parameter to be retrieved. The perturbed intensity, $I'(\tau,\Omega)$, should be considered in this case as the measured value at the optical depth τ and viewing direction Ω corresponding to an unknown value of the scalar parameter, c', whereas the intensity, $I(\tau,\Omega)$, is calculated employing an appropriate radiative transfer model for a known value of scalar parameter, c. Taking into account that in the case under consideration (6.5) contains only one unknown parameter, Δc, we obtain the following estimation for this scalar parameter:

$$\Delta c = \frac{\delta I(\tau,\Omega)}{\mathcal{V}_c(\tau,\Omega)} \quad\longrightarrow\quad c' = c + \frac{\delta I(\tau,\Omega)}{\mathcal{V}_c(\tau,\Omega)}\,, \tag{6.8}$$

where, according to its definition, $\Delta c = c' - c$.

Thus, the considered example demonstrates that the solution of a certain inverse problem requires not only the measured and simulated values of intensities but also an appropriate weighting function. However, a derivation of the weighting functions employing their definition according to Eqs (6.2) and (6.3) is possible in a few simplest cases only. Therefore, in the following sections we present an approach to derive weighting functions which allow us to avoid using Eqs (6.2) and (6.3). In particular, we consider how the weighting functions can be obtained employing the joint solution of the linearized radiative transfer equation (RTE) and the corresponding adjoint RTE.

6.3 Basic formulation of the direct and adjoint radiative transfer equations in the operator form

The derivation of the weighting functions presented below requires the formulation of the direct and adjoint radiative transfer equations in the so-called generalized form [25]. This representation as well as the adjoint approach used to derive analytical expressions for WFs will be briefly discussed below.

We start from the standard RTE for a plane-parallel scattering, absorbing, and emitting atmosphere illuminated by the incident solar radiation with the zenith angle θ_0. The irradiance flux is considered to be equal to $\pi\mu_0$ at the top of the medium, where $\mu_0 = \cos\theta_0$. The direct RTE can be written in the following form (see e.g. [4, 11, 12, 27] for derivation):

$$\mu\frac{\mathrm{d}I(\tau,\Omega)}{\mathrm{d}\tau} + I(\tau,\Omega) = J(\tau,\Omega) + (1-\omega(\tau))B(\tau)\,, \tag{6.9}$$

and appropriate boundary conditions are given by:

$$I(0,\Omega) \;=\; \pi\delta(\Omega-\Omega_0),\;\; \mu>0\,, \tag{6.10}$$

$$I(\tau_0,\Omega) \;=\; \frac{A}{\pi}\int_{\Omega_+}\rho(\Omega,\Omega')I(\tau_0,\Omega')\mu'\,\mathrm{d}\Omega' + \epsilon B(T_s),\;\; \mu<0\,, \tag{6.11}$$

where $J(\tau,\Omega)$ is the multiple scattering source function:

$$J(\tau,\Omega) = \frac{\omega(\tau)}{4\pi}\int_{4\pi} p(\tau,\Omega,\Omega')I(\tau,\Omega')\,\mathrm{d}\Omega'\,, \tag{6.12}$$

$\tau \in [0,\tau_0]$ is the optical depth, τ_0 is the optical thickness of the medium, $\omega(\tau) \in [0,1]$ is the single scattering albedo, $\mu \in [-1,1]$ is the cosine of the polar angle as measured from the positive τ-axis (i.e., negative values of μ correspond to the light propagated upwards), $\phi \in [0,2\pi]$ is the azimuthal angle, the variable $\Omega := \{\mu,\phi\}$ describes a set of variables $\mu \in [-1,1]$ and $\phi \in [0,2\pi]$, the variable $\Omega_+ := \{\mu,\phi\}$ describes the set of variables $\mu \in [0,1]$ and $\phi \in [0,2\pi]$, $\delta(\Omega-\Omega_0) = \delta(\mu-\mu_0)\delta(\phi-\phi_0)$ is the Dirac δ-function, $B(\tau)$ is the Planck function depending on the kinetic temperature of the medium, A is the spherical albedo of the underlying surface, $\rho(\Omega,\Omega')$ is a function determining the angular reflection properties of the boundary surface, ϵ is the surface emissivity, $B(T_s)$ is the Planck function at the surface temperature T_s, $p(\tau,\Omega,\Omega')$ is the phase function.

It is convenient to rewrite (6.9) and the corresponding boundary conditions given by (6.10) and (6.11) in the operator form. Let us define a linear differential-integral operator, L_e, which comprises all operations on the intensity $I(\tau,\Omega)$ in (6.9) as follows:

$$L_e = \mu\frac{d}{d\tau} + 1 - \frac{\omega(\tau)}{4\pi}\int_{4\pi}\mathrm{d}\Omega' p(\tau,\Omega,\Omega')\otimes\,, \tag{6.13}$$

where symbol $\otimes$ is used to denote an integral operator rather than a finite integral. The operator L_e is referred to as the direct radiative transfer operator. The radiative transfer equation is now written in the following operator form:

$$L_e\, I = S_e\,, \tag{6.14}$$

where

$$S_e \equiv S_e(\tau, \Omega) = [1 - \omega(\tau)]B(\tau)\,. \tag{6.15}$$

Although in the considered RTE the internal emission source function, $S_e(\tau, \Omega)$, is isotropic the argument Ω will be retained throughout this chapter for generality. To rewrite (6.10) and (6.11) in the operator form as well, we define two linear integral operators L_t and L_b as follows:

$$L_t = \int_0^{\tau_0} \mathrm{d}\tau\delta(\tau)\otimes\,, \tag{6.16}$$

$$L_b = \int_0^{\tau_0} \mathrm{d}\tau\delta(\tau - \tau_0)\left(\otimes - \frac{A}{\pi}\int_{4\pi} \mathrm{d}\Omega'\lambda(\mu')\rho(\Omega, \Omega')\otimes\right)\,. \tag{6.17}$$

Here, $\delta(\tau)$ and $\delta(\tau - \tau_0)$ are the Dirac δ-functions and $\lambda(\mu)$ is an auxiliary function introduced following [30] as $\lambda(\mu) = \mu\Theta(\mu)$, where $\Theta(\mu)$ is the Heaviside step-function over $\mu \in [-1, 1]$ given by

$$\Theta(\mu) = \begin{cases} 1, & \mu > 0 \\ 0, & \mu < 0 \end{cases}\,. \tag{6.18}$$

Operators L_t and L_b operate analogically to the operator L_e on the intensity $I(\tau, \Omega)$ and have the same domain. Thus, the operator form of the direct RTE alone with the boundary conditions is written as follows:

$$L_e I = S_e\,, \tag{6.19}$$

$$L_t I = S_t(\Omega),\ \mu > 0\,, \tag{6.20}$$

$$L_b I = S_b(\Omega),\ \mu < 0\,, \tag{6.21}$$

where according to (6.10) and (6.11)

$$S_t(\Omega) = \pi\delta(\Omega - \Omega_0)\,, \tag{6.22}$$

$$S_b(\Omega) = \epsilon B(T_s)\,. \tag{6.23}$$

The formulated direct RTE can be used to simulate the radiation field in a plane-parallel atmosphere in a wide spectral range from the ultraviolet to the thermal infrared. The polarization can be easily accounted for (see e.g. [6]).

6.3.1 Generalized form of the direct radiative transfer equation

The operator representation of the direct RTE and the corresponding boundary conditions formulated above describe a specific boundary value problem consisting of three independent operator equations. This boundary value problem can also be rewritten in the form of a single operator equation. Such representation is called the generalized form of the direct RTE. The generalized form of the direct RTE has been suggested by Ustinov [30] and its rigorous derivation has

been given by Rozanov and Rozanov [25] in the scalar case and by Rozanov [24] in the vector case (i.e., including polarization).

Following [25] the generalized form of the direct RTE is written as

$$LI = S\,. \tag{6.24}$$

Here, the generalized form of the direct radiative transfer operator, L, and the right-hand side, $S(\tau,\Omega)$, are determined as follows:

$$L = L_e + \psi_t(\tau,\mu)L_t + \psi_b(\tau,-\mu)L_b\,, \tag{6.25}$$

$$S(\tau,\Omega) = S_e(\tau,\Omega) + \psi_t(\tau,\mu)S_t(\Omega) + \psi_b(\tau,-\mu)S_b(\Omega)\,, \tag{6.26}$$

where auxiliary functions $\psi_t(\tau,\mu)$ and $\psi_b(\tau,-\mu)$ are given by

$$\psi_t(\tau,\mu) = \mu\delta(\tau)\Theta(\mu)\,, \tag{6.27}$$

$$\psi_b(\tau,-\mu) = -\mu\delta(\tau-\tau_0)\Theta(-\mu)\,. \tag{6.28}$$

The derived radiative transfer equation is equivalent to Eqs (6.19)–(6.21) but incorporate all operations with respect to the intensity at the boundaries, i.e., at this point, the boundary conditions are already included in the radiative transfer equation and do not need to be specified separately. This equation is the desired generalized form of the direct RTE containing all operations on the intensity field including boundary conditions.

6.3.2 Adjoint radiative transfer operator

Let B be a linear operator operating on a function $I(\tau,\Omega)$. Then according to its definition [9], the corresponding adjoint operator B^* has to satisfy the following identity:

$$(I^*, BI) = (B^*I^*, I)\,, \tag{6.29}$$

where the notation (,) denotes the scalar product in the appropriate functional space and $I^*(\tau,\Omega)$ is an arbitrary function which belongs to the domain of the operator B^*. Throughout this chapter we will assume that the scalar product of two arbitrary functions $f(\tau,\Omega)$ and $g(\tau,\Omega)$ is defined as follows:

$$(f,g) = \int_0^{\tau_0}\int_{4\pi} f(\tau,\Omega)g(\tau,\Omega)\,\mathrm{d}\tau\,\mathrm{d}\Omega\,. \tag{6.30}$$

Since the derivation of the adjoint radiative transfer operator using different approaches has already been described elsewhere [1,14,18,25,30], we will present just the final result here. Following [25], we write the expression for the adjoint radiative transfer operator in the following form:

$$L^* = L_e^* + \psi_t(\tau,-\mu)L_t^* + \psi_b(\tau,\mu)L_b^*\,, \tag{6.31}$$

where operators L_e^*, L_t^* and L_b^* are

$$L_e^* = -\mu\frac{d}{d\tau} + 1 - \frac{\omega(\tau)}{4\pi}\int_{4\pi} \mathrm{d}\Omega' p(\tau, \Omega', \Omega)\otimes\,, \tag{6.32}$$

$$L_t^* = \int_0^{\tau_0} \mathrm{d}\tau\delta(\tau)\otimes\,, \tag{6.33}$$

$$L_b^* = \int_0^{\tau_0} \mathrm{d}\tau\delta(\tau-\tau_0)\left[\otimes - \frac{A}{\pi}\int_{4\pi} \mathrm{d}\Omega'\rho(\Omega', \Omega)\lambda(-\mu')\otimes\right]\,. \tag{6.34}$$

Equation (6.31) is the desired generalized form of the adjoint radiative transfer operator. The adjoint operator, L^*, contains analogically to the direct operator, L, all operations on the adjoint intensity including boundary conditions.

6.3.3 Adjoint approach and the adjoint radiative transfer equation

In the previous subsection the generalized form of the adjoint radiative transfer operator has been presented. Here we will demonstrate how the adjoint radiative transfer equation can be formulated. We start from the generalized form of the direct RTE according to (6.24):

$$LI = S\,, \tag{6.35}$$

where S is given by (6.26). Assume we need to calculate a functional, say Φ, of the intensity I

$$\Phi = (W, I)\,, \tag{6.36}$$

where W is an arbitrary function of variables τ and Ω. There are two ways to solve this problem. One is to find the solution I of the direct RTE and apply (6.36) to calculate Φ (forward approach) and the other (adjoint approach) is to calculate the scalar product of both sides of (6.35) and an arbitrary function I^* and rewrite the left-hand side of the resulting equation using the definition of the adjoint operator, Eq. (6.29), as follows:

$$(I^*, LI) = (L^*I^*, I) = (I^*, S)\,. \tag{6.37}$$

Then, we obtain

$$(I^*, S) = (L^*I^*, I)\,. \tag{6.38}$$

If we require I^* to be the solution of the following adjoint equation:

$$L^*I^* = W\,, \tag{6.39}$$

equation (6.38) results in

$$(I^*, S) = (W, I) = \Phi\,. \tag{6.40}$$

Thus, the functional Φ can be found also as the scalar product of the solution of the adjoint RTE, I^*, and the right-hand side of the direct RTE written in the generalized form, S.

Similar to the forward boundary value problem defined by (6.35), Eq. (6.39) describes a boundary value problem for the adjoint intensity written in the generalized form. Operator L^* given by (6.31) includes the boundary conditions operators similar to the operator L given by (6.25). Thereby, similar to the right-hand side of the direct RTE, the right-hand side of the adjoint RTE given by (6.39) has to contain the boundary conditions as well. Thus, it should be possible to rewrite $W(\tau, \mu)$ in the following form:

$$W(\tau, \Omega) = W_e(\tau, \Omega) + \psi_t(\tau, -\mu) W_t(\Omega) + \psi_b(\tau, \mu) W_b(\Omega)\,, \tag{6.41}$$

where subscripts 'e', 't', and 'b' denote 'equation', upper ('top'), and lower ('bottom') boundary conditions, respectively. Substituting (6.41) into (6.39) we obtain the generalized form of the adjoint radiative transfer equation as follows:

$$L^* I^* = W_e + \psi_t(\tau, -\mu) W_t(\Omega) + \psi_b(\tau, \mu) W_b(\Omega)\,. \tag{6.42}$$

This equation can be treated in analogy to the generalized form of the direct RTE as a sum of three independent operator equations, namely, operator form of the adjoint RTE and boundary condition equations written in the operator form premultiplied by appropriate functions. Therefore, similar to the boundary value problem for the direct RTE, Eq. (6.42) can be separated into three equations as follows:

$$L_e^* I^* = W_e(\tau, \Omega)\,, \tag{6.43}$$

$$L_t^* I^* = W_t(\Omega)\,,\ \mu < 0\,, \tag{6.44}$$

$$L_b^* I^* = W_b(\Omega)\,,\ \mu > 0\ . \tag{6.45}$$

Equations (6.43)–(6.45) are referred to as the operator representation of the adjoint RTE. Substituting in these equations operators L_t^*, L_b^* and L_e^* as given by (6.33), (6.34) and (6.32), respectively, the standard form of the adjoint RTE can be formulated:

$$-\mu \frac{\mathrm{d}I^*(\tau, \Omega)}{\mathrm{d}\tau} + I^*(\tau, \Omega) = \frac{\omega}{4\pi} \int_{4\pi} p(\tau, \Omega', \Omega) I^*(\tau, \Omega')\, \mathrm{d}\Omega' + W_e(\tau, \Omega)\,, \tag{6.46}$$

$$I^*(0, \Omega) = W_t(\Omega),\ \ \mu < 0\,, \tag{6.47}$$

$$I^*(\tau_0, \mu) = W_b(\Omega) - \frac{A}{\pi} \int_{\Omega_-} \rho(\Omega', \Omega) I^*(\tau_0, \Omega') \mu'\, \mathrm{d}\Omega',\ \ \mu > 0\,. \tag{6.48}$$

We note that in contrast to the forward intensity the boundary conditions for the adjoint intensity are given for the outgoing adjoint radiation.

As clearly seen the adjoint and the direct RTEs are closely related to each other. Moreover, as demonstrated by many authors [1, 2, 15–17, 25] the solution of the adjoint RTE given by (6.46) can be found employing standard numerical methods developed for direct RTEs. Thereby, in fact, we do not need to develop special methods to solve the adjoint RTE.

6.4 General expressions for weighting functions

For the solution of most practical inverse problems a linear relationship between the measured functional of the radiative field and the atmospheric parameters is required. To obtain such a relationship let us formulate the measured functional as follows:

$$\Phi(\tau_v, \Omega_v) = (R, I) \equiv \int_0^{\tau_0} \int_{4\pi} R(\tau_v, \Omega_v; \tau, \Omega) I(\tau, \Omega)\, \mathrm{d}\tau\, \mathrm{d}\Omega\,, \tag{6.49}$$

where $R(\tau_v, \Omega_v; \tau, \Omega)$ is an instrument response function and a short notation for the scalar product as (,) is used. The specific form of the response function is of minor importance for our theoretical consideration. Therefore, following [30], we introduce the instrument response function appropriate to the instrument with an infinitesimally small field of view placed inside or at a boundary of a medium as follows:

$$R(\tau_v, \Omega_v; \tau, \Omega) = \delta(\tau - \tau_v)\delta(\Omega - \Omega_v)\,, \tag{6.50}$$

where $\delta(\Omega - \Omega_v) = \delta(\mu - \mu_v)\delta(\phi - \phi_v)$. The measured value, Φ, given by (6.49) is in this case the intensity of the radiation field at the optical depth $\tau = \tau_v$ in the direction $\Omega_v \equiv [\mu_v, \phi_v]$ characterized by the cosine of the zenith angle, μ_v, and azimuthal angle, ϕ_v.

Taking into account that the response function is independent of both atmospheric and surface parameters, the variation of the measured functional $\delta\Phi$ can be expressed as follows:

$$\delta\Phi(\tau_v, \Omega_v) = \Phi'(\tau_v, \Omega_v) - \Phi(\tau_v, \Omega_v) = (R, \delta I)\,, \tag{6.51}$$

where $\Phi'(\tau_v, \Omega_v)$ corresponds to the set of perturbed parameters. To express the scalar product in the right-hand side of (6.51) via the variation of the atmospheric and surface parameters we employ the adjoint approach. As discussed in section 6.3.3 the scalar product of the known function, R, and the function, δI, can be expressed as the scalar product of the adjoint intensity, I^*, and the right-hand side of the RTE describing the variation of the intensity, δI. To derive the corresponding RTE we rewrite following Marchuk [14] the direct RTE given by (6.24) for the perturbed values of the operator L', intensity I', and right-hand side S' :

$$L'I' = S'\,. \tag{6.52}$$

Here, the primed source function and the primed operator correspond in analogy to the primed intensity to the set of perturbed parameters. Substituting into this equation $I' = I + \delta I$, $L' = L + \delta L$ and $S' = S + \delta S$, we obtain

$$(L + \delta L)(I + \delta I) = S + \delta S \implies L\delta I + \delta L I + \delta L \delta I = \delta S\,. \tag{6.53}$$

In the linear approximation we can neglect the term containing the product $\delta L \delta I$. Therefore, the RTE describing the variation of intensity can be formulated in the following form:

$$L\delta I = \delta S - \delta L I\,. \tag{6.54}$$

Varying the operator L and the function S given by (6.25) and (6.26), respectively, and taking into account that the operator L_t and the function S_t as given by (6.16) and (6.22), respectively, are independent of the atmospheric and surface parameters, and therefore $\delta S_t = 0$ and $\delta L_t = 0$, we obtain the following expression for the right-hand side of (6.54):

$$\delta S - \delta L I = \sum_{p=1}^{P} \Big[(\delta_p S_e - \delta_p L_e I) + \psi_b(\tau, -\mu)(\delta_p S_b - \delta_p L_b I) \Big] , \qquad (6.55)$$

where P is the full number of parameters and δ_p denotes that the variation of the corresponding function or operator is caused by the variation of the parameter p only.

Variations of functions S_e and S_b as well as of operators L_e and L_b in the right-hand side of (6.55) can easily be expressed via the variation of the corresponding parameter $p_p(\tau)$ expanding them in the Taylor series with respect to this parameter and restricting with the linear term relative to $\delta p_p(\tau)$. For example, for the function S_e we obtain

$$\delta_p S_e(\tau, \Omega) = S'_e(\tau, \Omega) - S_e(\tau, \Omega) = \frac{\partial S_e(\tau, \Omega)}{\partial p_p(\tau)} \delta p_p(\tau) , \qquad (6.56)$$

where $S'_e(\tau, \Omega)$ is the source function for the perturbed parameter $p'_p(\tau)$ and $\partial S_e(\tau, \Omega)/\partial p_p(\tau)$ is the partial derivative of the function $S_e(\tau, \Omega)$ with respect to the parameter $p_p(\tau)$.

Employing Eq. (6.56) and introducing the relative variation of the corresponding parameter as $v_p(\tau) = \delta p_p(\tau)/p_p(\tau)$, the terms in the right-hand side of (6.55) can be rewritten in the linear approximation as follows:

$$\delta_p S_e - \delta_p L_e I = \left[\frac{\partial S_e(\tau, \Omega)}{\partial p_p(\tau)} - \frac{\partial L_e}{\partial p_p(\tau)} I \right] \delta p_p(\tau) = v_p(\tau) Y_p(\tau, \Omega) , \qquad (6.57)$$

$$\delta_p S_b - \delta_p L_b I = \left[\frac{\partial S_b(\Omega)}{\partial p_p(\tau)} - \frac{\partial L_b}{\partial p_p(\tau)} I \right] \delta p_p(\tau) = v_p(\tau) G_p(\Omega) , \qquad (6.58)$$

where functions $Y_p(\tau, \Omega)$ and $G_p(\Omega)$ contain partial derivatives of the appropriate functions and operators:

$$Y_p(\tau, \Omega) = p_p(\tau) \left[\frac{\partial S_e(\tau, \Omega)}{\partial p_p(\tau)} - \frac{\partial L_e}{\partial p_p(\tau)} I \right] , \qquad (6.59)$$

$$G_p(\Omega) = p_p(\tau) \left[\frac{\partial S_b(\Omega)}{\partial p_p(\tau)} - \frac{\partial L_b}{\partial p_p(\tau)} I \right] . \qquad (6.60)$$

Introducing an auxiliary function $\Psi_p(\tau, \Omega)$ as

$$\Psi_p(\tau, \Omega) = Y_p(\tau, \Omega) + \psi_b(\tau, -\mu) G_p(\Omega) \qquad (6.61)$$

and substituting it into the right-hand side of (6.55), we obtain

$$\delta S - \delta L I = \sum_{p=1}^{P} v_p(\tau) \Psi_p(\tau, \Omega) \,. \tag{6.62}$$

We note that for a scalar parameter we only need to replace $v_p(\tau)$ by v_c, where $v_c = \Delta c/c$ is the relative variation of this parameter. Therefore, this case does not need to be considered separately. Substituting further (6.62) into the right-hand side of (6.54), we have

$$L\delta I = \sum_{p=1}^{P} v_p(\tau) \Psi_p(\tau, \Omega) \,. \tag{6.63}$$

Equation (6.63) provides a linear relationship between the variation of the intensity and the relative variations of the atmospheric and surface parameters. This equation will be referred to as the generalized form of the linearized direct radiative transfer equation (LRTE).

Multiplying both sides of the LRTE given by (6.63) by an arbitrary function $I^*(\tau, \Omega)$ and using the definition of the adjoint operator as given by (6.29), we obtain

$$\left(I^*, L\delta I\right) = \left(L^* I^*, \delta I\right) = \left(I^*, \sum_{p=1}^{P} v_p(\tau) \Psi_p\right) . \tag{6.64}$$

Let us require now that the function $I^*(\tau, \Omega)$ is the solution of the following linear operator equation:

$$L^* I^* = R \,, \tag{6.65}$$

where R is the response function given by (6.50). Then, substituting the response function R instead of $L^* I^*$ into (6.64), we obtain the expression for the variation of the measured functional $\delta\Phi(\tau_v, \Omega_v) = (R, \delta I)$ as the scalar product of the adjoint intensity, I^*, and the right-hand side of LRTE given by (6.63):

$$\delta\Phi(\tau_v, \Omega_v) = (R, \delta I) = \left(I^*, \sum_{p=1}^{P} v_p(\tau) \Psi_p \right) . \tag{6.66}$$

Thus, we have obtained the desired linear relationship between the variation of the measured functional and variations of the atmospheric and surface parameters. We note that the adjoint intensity, I^*, as a solution of (6.65) is a function of variables τ and Ω and depends parametrically on variables τ_v and Ω_v describing the position and direction of observation, i.e., $I^* \equiv I^*(\tau, \Omega; \tau_v, \Omega_v)$. However, for simplicity the explicit notation of the dependence of the adjoint intensity on the observation position, τ_v, will be omitted in the following discussion.

Introducing a short notation for the integral of the product of two arbitrary functions $f(\tau, \Omega)$ and $g(\tau, \Omega)$ over Ω as

$$\int_{4\pi} f(\tau, \Omega) g(\tau, \Omega) \, \mathrm{d}\Omega \equiv \langle f g \rangle \,, \tag{6.67}$$

and taking into account that the scalar product is defined according to (6.30), the variation of the measured functional $\delta\Phi$ as given by (6.66) can be rewritten as follows:

$$\delta\Phi(\tau_v, \Omega_v) = \sum_{p=1}^{P} \int_0^{\tau_0} \langle \Psi_p I^* \rangle \, v_p(\tau) \, \mathrm{d}\tau \,. \tag{6.68}$$

Thus, in the case of one scalar parameter, c, and one parameter-function, $p(\tau)$, we obtain

$$\delta\Phi(\tau_v, \Omega_v) = v_c \int_0^{\tau_0} \langle \Psi_c I^* \rangle \, \mathrm{d}\tau + \int_0^{\tau_0} \langle \Psi_p I^* \rangle \, v_p(\tau) \, \mathrm{d}\tau \,. \tag{6.69}$$

Comparing this equation to (6.6), we conclude that the weighting functions for a scalar parameter and for a parameter-function can be written as

$$\mathcal{W}_c(\tau_v, \Omega_v) = \int_0^{\tau_0} \left\langle \Psi_c I^* \right\rangle \mathrm{d}\tau \equiv \int_0^{\tau_0} \int_{4\pi} \Psi_c(\tau, \Omega) I^*(\tau, \Omega; \Omega_v) \, \mathrm{d}\Omega \, \mathrm{d}\tau \tag{6.70}$$

and

$$\mathcal{W}_p(\tau; \tau_v, \Omega_v) = \left\langle \Psi_p I^* \right\rangle \equiv \int_{4\pi} \Psi_p(\tau, \Omega) I^*(\tau, \Omega; \Omega_v) \, \mathrm{d}\Omega \,, \tag{6.71}$$

respectively. Here, functions $\Psi_c(\tau, \Omega)$ and $\Psi_p(\tau, \Omega)$ are given by (6.61) and the adjoint intensity, $I^*(\tau, \Omega; \Omega_v)$, is the solution of the adjoint RTE given by (6.65).

The derived WFs for the parameter-functions provide a linear relationship between the variation of the intensity at a given position and direction and the variation of a certain optical parameter at any point inside the medium. Equatioins (6.70) and (6.71) signify the importance of the adjoint intensity, $I^*(\tau, \Omega)$, for the calculations of the weighting functions and, therefore, for the solution of inverse problems.

Although Eqs (6.59)–(6.61) can be used to obtain analytical expressions for the auxiliary functions $\Psi_p(\tau, \Omega)$ and, thus, for the corresponding weighting functions, for any desired parameter, in practice only the analytical expressions for the weighting functions with respect to the directly involved in the formulated RTE parameters are required whereas WFs for all other parameters can be obtained as a linear combination of the weighting functions for these main parameters. In the case under consideration main parameter-functions are the extinction coefficient, single scattering albedo and kinetic temperature of the medium, and the scalar parameters are the surface albedo, surface emissivity and surface temperature, whereas secondary parameter-functions whose weighting functions can be obtained as a linear combination of the main parameter WFs mentioned above are, for example, the scattering and absorption coefficients. For this reason, only the analytical expressions for auxiliary functions corresponding to the main parameters are presented in the Appendix.

6.5 Weighting functions for absorption and scattering coefficients

The expressions for the extinction coefficient and the single scattering albedo weighting functions derived in the Appendix (see Eqs (6.240) and (6.244), respectively) allow us to formulate the weighting functions for the scattering and absorption coefficients as well. Indeed, assuming that both extinction coefficient and single scattering albedo are varying simultaneously, we can write

$$\delta\phi(\tau;\tau_v,\Omega_v) = \mathcal{W}_e(\tau;\tau_v,\Omega_v)v_e(\tau) + \mathcal{W}_\omega(\tau;\tau_v,\Omega_v)v_\omega(\tau)\,, \tag{6.72}$$

where $\delta\phi(\tau;\tau_v,\Omega_v)\,\mathrm{d}\tau$ can be considered as the contribution of the extinction coefficient and single scattering albedo variations within an infinitesimal layer positioned at the optical depth τ, into the variation of the measured functional, $\delta\Phi(\tau_v,\Omega_v)$, i.e.,

$$\delta\Phi(\tau_v,\Omega_v) = \int_0^{\tau_0} \delta\phi(\tau;\tau_v,\Omega_v)\,\mathrm{d}\tau\,. \tag{6.73}$$

The relative variations $v_e(\tau)$ and $v_\omega(\tau)$ can be caused by variations of the absorption and/or scattering coefficients, namely

$$v_e(\tau) = v_s(\tau)\omega(\tau) + v_a(\tau)[1-\omega(\tau)]\,, \tag{6.74}$$

$$v_\omega(\tau) = [v_s(\tau) - v_a(\tau)][1-\omega(\tau)]\,, \tag{6.75}$$

where $\omega(\tau)$ is the single scattering albedo and the relative variations of the scattering and absorption coefficients ($\sigma_s(\tau)$ and $\sigma_a(\tau)$, respectively) are given by $v_s(\tau) = \delta\sigma_s(\tau)/\sigma_s(\tau)$ and $v_a(\tau) = \delta\sigma_a(\tau)/\sigma_a(\tau)$, respectively. Substituting $v_e(\tau)$ and $v_\omega(\tau)$ according to (6.74) and (6.75) into (6.72) and introducing functions $\mathcal{W}_a$ and $\mathcal{W}_s$ as follows:

$$\mathcal{W}_a(\tau;\tau_v,\Omega_v) = \big[\mathcal{W}_e(\tau;\tau_v,\Omega_v) - \mathcal{W}_\omega(\tau;\tau_v,\Omega_v)\big]\big[1-\omega(\tau)\big]\,, \tag{6.76}$$

$$\mathcal{W}_s(\tau;\tau_v,\Omega_v) = \mathcal{W}_e(\tau;\tau_v,\Omega_v)\omega(\tau) + \mathcal{W}_\omega(\tau;\tau_v,\Omega_v)[1-\omega(\tau)]\,, \tag{6.77}$$

we have

$$\delta\phi(\varpi_v,\tau) = \mathcal{W}_a(\tau;\tau_v,\Omega_v)v_a(\tau) + \mathcal{W}_s(\tau;\tau_v,\Omega_v)v_s(\tau)\,. \tag{6.78}$$

Thus, functions $\mathcal{W}_a(\tau;\tau_v,\Omega_v)$ and $\mathcal{W}_s(\tau;\tau_v,\Omega_v)$ defined by (6.76) and (6.77) are the weighting functions for the absorption and scattering coefficients, respectively. As pointed out in the previous section, these WFs are expressed as a linear combination of the corresponding WFs for the extinction coefficient and the single scattering albedo.

6.6 Weighting functions for a mixture of scattering and absorbing components

In the previous sections we have derived the expressions for the weighting functions appropriate to the direct RTE formulated for the extinction coefficient and the single scattering albedo as two independent variables. In this section we extend the derived expressions for the case of a mixture of the scattering and absorbing components. This is of great importance for the Earth's atmosphere, where the solar radiation can be scattered by the molecules, aerosol particles, or cloud droplets and it be absorbed by various gases. The scattering and the extinction coefficients are defined in this case as follows:

$$\sigma_s(\tau) = \sum_{i=1}^{N_s} s_i(\tau)\,, \tag{6.79}$$

$$\sigma_e(\tau) = \sigma_s(\tau) + \sum_{k=1}^{N_a} a_k(\tau)\,, \tag{6.80}$$

where $s_i(\tau)$ is the scattering coefficient for the ith component, N_s is the number of the scattering components, $a_k(\tau)$ is the kth absorption coefficient, and N_a is the number of absorbing components including the absorption by aerosol, gases and clouds. The probability of the photon scattering on the ith component can now be defined as follows:

$$\omega_i(\tau) = \frac{s_i(\tau)}{\sigma_e(\tau)}\,. \tag{6.81}$$

This probability will be referred to as the partial single scattering albedo. Taking into account that each sort of the scattering components has its phase function, the radiative transfer operator, L_e, given by (6.13) should be rewritten as follows:

$$L_e = \mu\frac{\mathrm{d}}{\mathrm{d}\tau} + 1 - \sum_{i=1}^{N_s}\frac{\omega_i(\tau)}{4\pi}\int_{4\pi}\mathrm{d}\Omega' p_i(\tau,\Omega,\Omega')\otimes\,, \tag{6.82}$$

where $p_i(\tau,\Omega,\Omega')$ is the phase function appropriate to the ith scattering component. Assuming that the scattering processes on the different components are independent, we do not need any additional modification to describe the radiative transfer in the medium consisting of a mixture of the scattering and absorbing particles.

To modify the derived expressions for WFs, we consider the extinction coefficient and the partial single scattering albedos to be main parameter-functions. Although the expression for the extinction coefficient WF remains the same as given by (6.240), the multiple scattering source function, $J(\tau,\Omega)$, consists now of a sum of the multiple scattering source functions for all scattering components:

$$J(\tau,\Omega) = \sum_{i=1}^{N_s} J_i(\tau,\Omega) = \sum_{i=1}^{N_s}\frac{\omega_i(\tau)}{4\pi}\int_{4\pi} p_i(\tau,\Omega,\Omega')I(\tau,\Omega')\,\mathrm{d}\Omega'\,. \tag{6.83}$$

Thus, the expression for the extinction coefficient WF can be written as follows:

$$\mathcal{W}_e(\tau;\tau_v,\Omega_v) = \int_{4\pi} I^*(\tau,\Omega;\Omega_v)\Big[J(\tau,\Omega) + S_e(\tau,\Omega) - I(\tau,\Omega)\Big]\,\mathrm{d}\Omega\,, \quad (6.84)$$

where $J(\tau,\Omega)$ is given by (6.83).

The WF for the partial single scattering albedo, $\omega_i(\tau)$, can be derived in a way analogical to the derivation of the WF for the single scattering albedo in the case of one scattering component. Considering $\omega_i(\tau)$ as an independent variable, the result can be written in the form of Eq. (6.244) as follows:

$$\mathcal{W}_{\omega_i}(\tau;\tau_v,\Omega_v) = \int_{4\pi} I^*(\tau,\Omega;\Omega_v)\Big[J_i(\tau,\Omega) - B(\tau)\omega_i(\tau)\Big]\,\mathrm{d}\Omega\,. \quad (6.85)$$

Let us now derive WF for the absorption coefficient and the scattering coefficient of the kth component. Assuming that the extinction coefficient and all partial single scattering albedos are varying, we can write

$$\delta\phi(\tau;\tau_v,\Omega_v) = \mathcal{W}_e(\tau;\tau_v,\Omega_v)v_e(\tau) + \sum_{i=1}^{N_s}\mathcal{W}_{\omega_i}(\tau;\tau_v,\Omega_v)v_{\omega_i}(\tau)\,, \quad (6.86)$$

where $\delta\phi(\tau;\tau_v,\Omega_v)\,\mathrm{d}\tau$ is the contribution of the extinction coefficient and the partial single scattering albedo variations within an infinitesimal layer positioned at the optical depth τ, into the variation of the measured functional, $\delta\Phi(\tau_v,\Omega_v)$, as given by (6.73), and $v_{\omega_i}(\tau)$ is the relative variation of the ith partial single scattering albedo, i.e., $v_{\omega_i}(\tau) = \delta\omega_i(\tau)/\omega_i(\tau)$. Varying the extinction coefficient, $\sigma_e(\tau)$, and the partial single scattering albedo, $\omega_i(\tau)$, with respect to the kth absorption coefficient, we obtain

$$v_e(\tau) = \frac{\delta_k\sigma_e(\tau)}{\sigma_e(\tau)} = \frac{a_k(\tau)}{\sigma_e(\tau)}v_{a_k}(\tau)\,, \quad (6.87)$$

$$v_{\omega_i}(\tau) = \frac{1}{\omega_i(\tau)}\delta_k\left[\frac{s_i(\tau)}{\sigma_e(\tau)}\right] = -\frac{a_k(\tau)}{\sigma_e(\tau)}v_{a_k}(\tau)\,, \quad (6.88)$$

where $v_{a_k}(\tau) = \delta a_k(\tau)/a_k(\tau)$. Substituting (6.87) and (6.88) into (6.86), we have

$$\delta_k\phi(\tau;\tau_v,\Omega_v) = \left[\mathcal{W}_e(\tau;\tau_v,\Omega_v) - \sum_{i=1}^{N_s}\mathcal{W}_{\omega_i}(\tau;\tau_v,\Omega_v)\right]\frac{a_k(\tau)}{\sigma_e(\tau)}v_{a_k}(\tau)\,. \quad (6.89)$$

Introducing the WF for the single scattering albedo, $\omega(\tau) = \sum\omega_i(\tau)$, as follows:

$$\mathcal{W}_\omega(\tau;\tau_v,\Omega_v) = \sum_{i=1}^{N_s}\mathcal{W}_{\omega_i}(\tau;\tau_v,\Omega_v)\,, \quad (6.90)$$

and taking into account (6.85) for the partial single scattering albedo WF, we have

$$\mathcal{W}_\omega(\tau;\tau_v,\Omega_v)=\int_{4\pi} I^*(\tau,\Omega;\Omega_v)\Big[J(\tau,\Omega)-B(\tau)\omega(\tau)\Big]\,\mathrm{d}\Omega\,, \tag{6.91}$$

where the multiple scattering source function, $J(\tau,\Omega)$, is given by (6.83) and $\omega(\tau)$ is the single scattering albedo. Thus, the expression for the kth absorption coefficient WF can be written in the following form:

$$\mathcal{W}_{a_k}(\tau;\tau_v,\Omega_v)=\frac{a_k(\tau)}{\sigma_e(\tau)}\Big[\mathcal{W}_e(\tau;\tau_v,\Omega_v)-\mathcal{W}_\omega(\tau;\tau_v,\Omega_v)\Big]\,. \tag{6.92}$$

In an analogous way we can derive the expression for the kth scattering coefficient WF. Indeed, varying now the extinction coefficient, $\sigma_e(\tau)$, and the partial single scattering albedo, $\omega_i(\tau)$, with respect to the kth scattering coefficient, we obtain

$$v_e(\tau)=\omega_k(\tau)v_{s_k}(\tau)\,, \tag{6.93}$$

$$v_{\omega_i}(\tau)=-\omega_k(\tau)v_{s_k}(\tau),\ i\neq k\,, \tag{6.94}$$

$$v_{\omega_k}(\tau)=v_{s_k}(\tau)-\omega_k(\tau)v_{s_k}(\tau),\ i=k\,, \tag{6.95}$$

where $v_{s_k}(\tau)=\delta s_k(\tau)/s_k(\tau)$.

Substituting (6.93)–(6.95) into (6.86), we have

$$\begin{aligned}\delta_k\phi(\tau;\tau_v,\Omega_v) \;=\; & \left[\mathcal{W}_e(\tau;\tau_v,\Omega_v)-\sum_{i=1}^{N_s}\mathcal{W}_{\omega_i}(\tau;\tau_v,\Omega_v)\right]\omega_k(\tau)v_{s_k}(\tau)\\ +\; & \mathcal{W}_{\omega_k}(\tau;\tau_v,\Omega_v)v_{s_k}(\tau)\,.\end{aligned} \tag{6.96}$$

Thus, the expression for the kth scattering coefficient WF can be written in the following form:

$$\begin{aligned}\mathcal{W}_{s_k}(\tau;\tau_v,\Omega_v) \;=\; & \omega_k(\tau)\Big[\mathcal{W}_e(\tau;\tau_v,\Omega_v)-\mathcal{W}_\omega(\tau;\tau_v,\Omega_v)\Big]\\ +\; & \mathcal{W}_{\omega_k}(\tau;\tau_v,\Omega_v)\,.\end{aligned} \tag{6.97}$$

Here, functions $\mathcal{W}_e$, $\mathcal{W}_{\omega_k}$, and $\mathcal{W}_\omega$ are given by (6.84), (6.85), and (6.91), respectively. Thus, we can see that also for a mixture of scattering and absorbing components the weighting functions for the scattering and absorption coefficients of each particle type can be expressed as a linear combination of WF derived for the main parameter-functions.

6.7 Examples of weighting functions for the aerosol and cloud parameters

In this section we compare the weighting functions for the absorption and scattering coefficients of the aerosol particles and for the scattering coefficient of the water droplets calculated according to the analytical expressions given by (6.92) and (6.97) to WFs obtained employing the numerical perturbation approach.

We will assume here that the measured functional, $\Phi(\tau_v, \Omega_v)$, is the intensity of the reflected radiation at the top of atmosphere (TOA) in the nadir direction. As pointed out in section 6.2, the WF for the absolute variation of a certain atmospheric parameter corresponds to the variational derivative of the intensity with respect to this parameter. Therefore, the WF can be calculated directly according to the definition of the variational derivative given by (6.3). Employing the finite-difference approximation, this expression can be rewritten as follows:

$$\mathcal{V}_p(\tau_i; \tau_v, \Omega_v) \approx \frac{I[\tau_v, \Omega_v; p(\tau) + \Delta p(\tau_i)] - I[\tau_v, \Omega_v; p(\tau)]}{\Delta p(\tau_i)}\,, \tag{6.98}$$

where $I[\tau_v, \Omega_v; p(\tau)]$ and $I[\tau_v, \Omega_v; p(\tau) + \Delta p(\tau_i)]$ are the unperturbed and perturbed intensities at the optical depth τ_v in direction Ω_v and $\Delta p(\tau_i)$ is the perturbation of the parameter $p(\tau)$ at the altitude level τ_i. Equation (6.98) provides the finite-difference approximation for the variational derivative and, therefore, for the weighting function at an altitude level with the optical depth τ_i. Assuming that the entire atmosphere is divided into $N-1$ layers, WF can be obtained for all altitude levels successively employing (6.98) for $i = 1, \ldots, N$. Thus, WFs for all discrete levels can be obtained running the radiative transfer model once for the unperturbed value of the desired parameter and subsequently N times to account for parameter perturbations at all discrete altitude levels:

$$p_i(\tau) = p(\tau) + \Delta p(\tau_i),\ i = 1, \ldots, N\,. \tag{6.99}$$

Weighting functions calculated according to the described approach will be referred to as the numerical weighting functions.

It is worth noting that numerical WFs calculated according to (6.98) cannot be directly compared to the analytical WFs resulting from, for example, Eq. (6.97). The main reason for this is as follows. Any numerical method of solving the radiative transfer equation assumes a certain distribution of optical parameters within each discrete layer in the atmosphere and this distribution is based on the values specified at the boundaries of layers, i.e., at internal discretization levels. For this reason, a perturbation of the parameter $p(\tau)$ at an altitude level corresponding to the optical depth τ_i affects the vertical distribution of this parameter in both upper and lower layers having their boundary at this altitude, i.e., effectively the vertical distribution of the parameter is perturbed within two layers. Thus, the numerical WFs describe the variation of the intensity caused by the variation of the optical parameter within two altitude layers having a finite geometrical and optical thicknesses, whereas the analytical WFs describe the intensity variation caused by the variation of the parameter in an infinitesimally thin altitude layer. Therefore, to compare the numerical and analytical WFs we introduce the layer-integrated analytical WF corresponding to the variation of the parameter $p(\tau)$ at the discrete level τ_i as follows:

$$\mathcal{W}_p(\tau_i; \tau_v, \Omega_v) = \frac{1}{2}\int_{\tau_{i-1}}^{\tau_{i+1}} \mathcal{W}_p(\tau; \tau_v, \Omega_v)\,\mathrm{d}\tau\,, \tag{6.100}$$

where the integration is performed over two neighboring layers bordered by the altitude level τ_i.

Although the computation of the numerical WFs employing (6.98) is very time-consuming, they are often needed to prove the correctness of the derivation and of the numerical implementation of the corresponding analytical expressions.

6.7.1 Weighting functions for the aerosol scattering coefficient and aerosol particles number density

At first we compare the numerical and the layer-integrated analytical WFs for the aerosol scattering coefficient in the O_2-A absorption band (spectral range 758–773 nm). The vertical profiles of the aerosol extinction coefficient and of the aerosol single scattering albedo used in calculations are presented in Fig. 6.1. The profiles are shown at 758 nm wavelength. The phase function of the aerosol particles was reperesented by the Heney–Greenstein phase function with a constant asymmetry parameter of 0.67.

According to the definition of the layer-integrated WFs the variation of the aerosol scattering coefficient, $\Delta s_a(\tau_i)$, at the level τ_i causes the variation of the intensity at the optical depth τ_v in the direction Ω_v which can be expressed as follows:

$$\Delta_i I(\tau_v, \Omega_v) = \mathcal{W}_{s_a}(\tau_i; \tau_v, \Omega_v) v_{s_a}(\tau_i)\,. \tag{6.101}$$

Here, $\mathcal{W}_{s_a}(\tau_i; \tau_v, \Omega_v)$ is the layer-integrated WF for the aerosol scattering coefficient and $v_{s_a}(\tau_i)$ is its relative variation. Dividing both sides of this equation

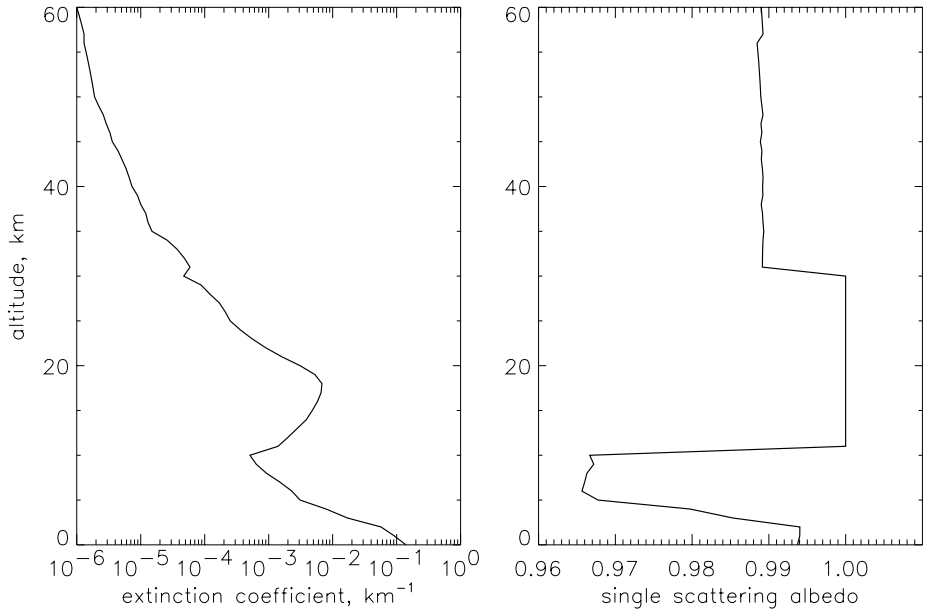

Fig. 6.1. Vertical profiles of the aerosol extinction coefficient (left panel) and of the aerosol single scattering albedo (right panel) used in the comparison of the weighting functions.

by the intensity $I(\tau_v, \Omega_v)$, we obtain

$$\frac{\Delta_i I(\tau_v, \Omega_v)}{I(\tau_v, \Omega_v)} = \frac{\mathcal{W}_{s_a}(\tau_i; \tau_v, \Omega_v)}{I(\tau_v, \Omega_v)} v_{s_a}(\tau_i) = \mathcal{R}_{s_a}(\tau_i; \tau_v, \Omega_v) v_{s_a}(\tau_i)\,. \qquad (6.102)$$

Thus, assuming 1% variation of the aerosol scattering coefficient, $v_{s_a}(\tau_i)$, within a layer with a geometrical thickness $\Delta_i z = z_{i+1} - z_{i-1}$, the percentage variation of the intensity becomes numerically equivalent to the normalized layer-integrated WF, $\mathcal{R}_{s_a}(\tau_i; \tau_v, \Omega_v)$.

Comparisons of the numerical and the normalized layer-integrated analytical WFs for the aerosol scattering coefficient in the monochromatic case at selected wavelengths within the O_2-A absorption band are shown in Fig. 6.2. The numerical WFs were calculated assuming the relative variation of the aerosol scattering coefficient to be 0.01% at each atmospheric level. The entire atmosphere between 0 and 60 km was divided into 60 layers. As seen from the plot the shape and the maximum value of WFs are strongly dependent on the gaseous absorption. At very week absorption ($\tau_g = 0.006$ in Fig. 6.2) the maximum of WF is located near the surface and the maximum value is about 0.004%. An enhanced gaseous absorption causes the second maximum in the altitude region of the stratospheric aerosol layer (∼18 km, see Fig. 6.1) to appear. Further increase in the optical

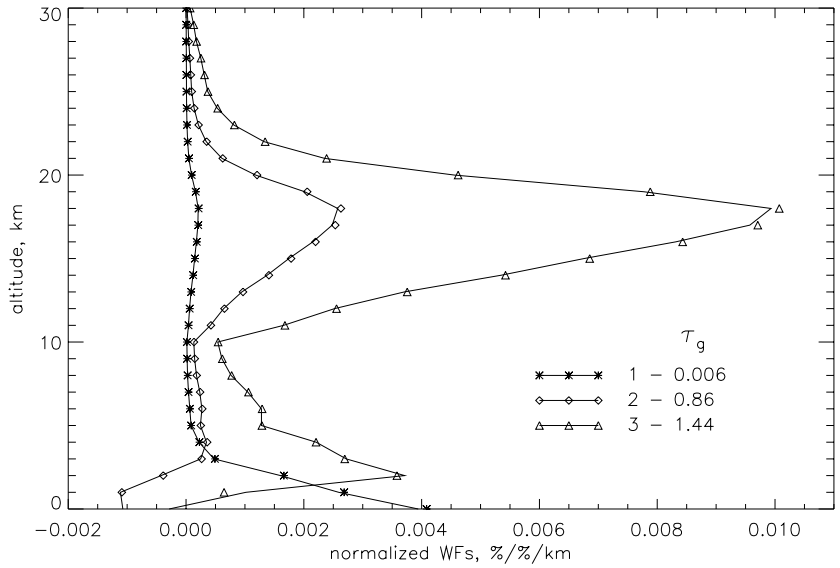

Fig. 6.2. Comparison of the numerical (symbols) and the normalized layer-integrated analytical WFs (solid line) for the aerosol scattering coefficient at selected wavelengths within the O_2-A absorption band: 1, 758.2 nm; 2, 763.8 nm; 3, 760.055 nm. The optical thicknesses of gaseous absorbers (τ_g) at these wavelengths is shown in the legend. The weighting functions were calculated for the monochromatic reflected intensity at TOA observed in the nadir viewing geometry at a solar zenith angle of 45°. The surface albedo was set to 0.3.

thickness of the gaseous absorber to 1.44 raises the lower maximum of the WF and increases the value of the upper maximum to about 0.01%.

Obtained results demonstrate that spectral measurements of the reflected intensity within the absorptions bands of atmospheric gases, e.g., O_2-A band, contain certian information about the vertical distribution of the aerosol optical parameters. To illustrate this we consider more realistic case of measurements of the reflected solar radiance at TOA in the entire O_2-A absorption band with a finite spectral resolution. The instrument slit function is approximated by the boxcar function with a full width of 0.05 nm. The corresponding spectrum of the reflected solar radiance observed at TOA in nadir viewing geometry is shown in Fig. 6.3. The intensity were simulated assuming the incident solar flux at TOA to be equal π. This intensity is closely related to the reflection function, R, defined as follows:

$$R = \frac{\pi I}{\mu_0 F}\,, \tag{6.103}$$

where I is the intensity of radiation, F is the incident solar flux, and μ_0 is the cosine of the solar zenith angle. If the incident solar flux, F, is assumed to be equal π as mentioned above, the following relationship between the reflection function and the intensity is obtained:

$$R = \frac{I}{\mu_0}\,. \tag{6.104}$$

The variations of the aerosol scattering and absorption coefficients are caused in particular by the variation of the aerosol particles number density, $N_a(\tau)$.

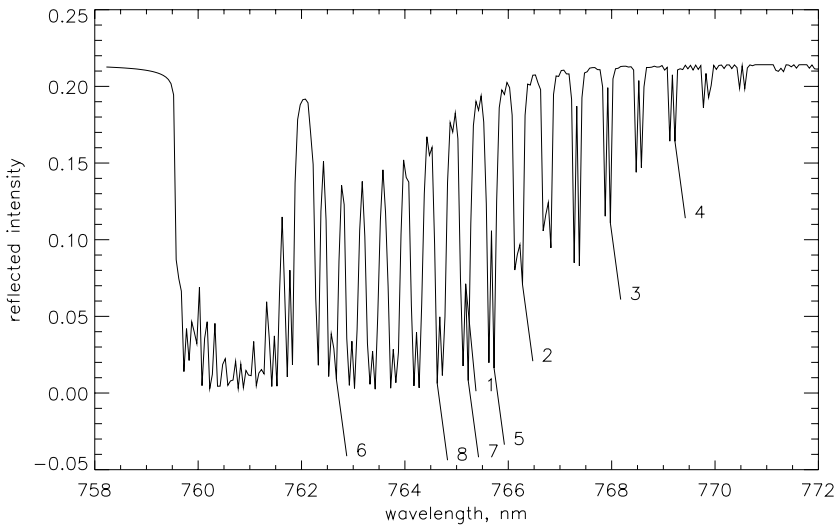

Fig. 6.3. Reflected solar radiation in the O_2-A absorption band spectral range observed at TOA in the nadir viewing geometry at a solar zenith angle of 45°. The surface albedo was set to 0.3. The wavelengths selected for presentation of the weighting functions in Fig. 6.4 are marked by the numbers.

Their relative variations can be expressed via the variation of $N_a(\tau)$ as follows:

$$\frac{\delta s_a(\tau)}{s_a(\tau)} = \frac{\delta N_a(\tau)}{N_a(\tau)} \quad \text{and} \quad \frac{\delta a_a(\tau)}{a_a(\tau)} = \frac{\delta N_a(\tau)}{N_a(\tau)}\,. \tag{6.105}$$

Since a variation of the aerosol particles number density leads to variations of both aerosol scattering and absorption coefficients, the corresponding weighting function has to be given by a linear combination of the aerosol scattering and absorption coefficient WFs, namely, taken into account (6.105), by their sum:

$$\mathcal{W}_{N_a}(\tau;\tau_v,\Omega_v) = \mathcal{W}_{s_a}(\tau;\tau_v,\Omega_v) + \mathcal{W}_{a_a}(\tau;\tau_v,\Omega_v)\,. \tag{6.106}$$

Figure 6.4 shows the normalized layer-integrated WFs for the aerosol particle number density at selected wavelengths within the O_2-A absorption band. As can be clearly seen, the shape and the maximum value of WFs are strongly dependend on the optical thickness of the gaseous absorber. For example, in a case of a weak gaseous absorption, $\tau_g \lesssim 6$, (left panel in Fig. 6.4) the maxima of the WFs are located in the lower troposphere and 1% variation in the particle number density within the boundary layer causes the variation of the reflected intensity in the range from -0.0015% to $+0.002\%$ depending on τ_g. In the spectral channels characterized by a stronger gaseous absorption, $\tau_g \gtrsim 9$, (right panel in Fig. 6.4) WFs have their maxima in the altitude region of the

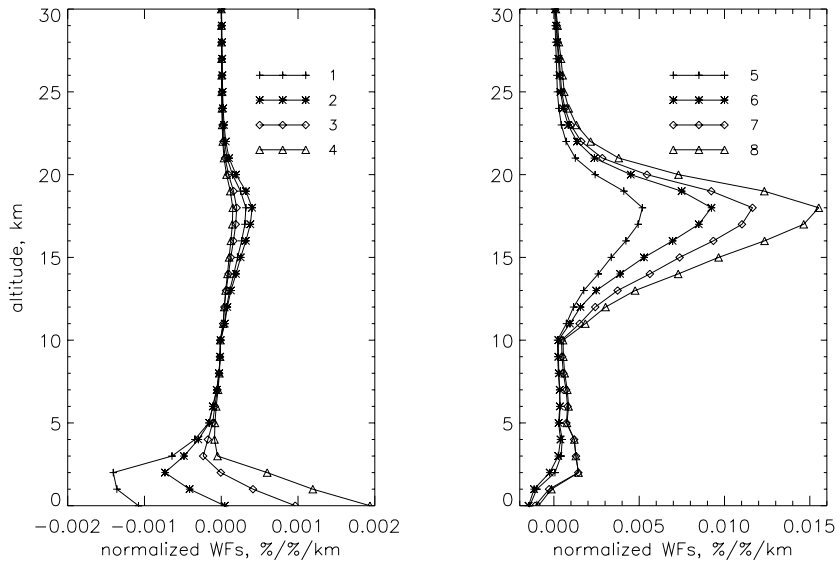

Fig. 6.4. Normalized layer-integrated WFs for the aerosol particle number density at selected wavelengths within the O_2-A absorption band. The optical thicknesses of gaseous absorbers at these wavelengths is: 1, 0.5; 2, 5.5; 3, 1.1; 4, 0.2; 5, 9.1; 6, 28.5; 7, 14.2; 8, 17.5. The weighting functions were calculated for the reflected intensity at TOA observed in the nadir viewing geometry at a solar zenith angle of 45°. The surface albedo was set to 0.3.

stratospheric aerosol layer (∼18 km). The sensitivity of the reflected radiance to the variation of the stratospheric aerosol particles concentration is much higher than in the case of the boundary layer aerosol. For example, 1% variation of the aerosol number density at the altitude of about 18 km causes a relative variation of the reflected intensity at the TOA of about 0.015% in a spectral channel with $\tau_g = 17.5$.

A quick look analysis of the vertical behavior of the aerosol number density WFs shows that their maxima are located at 0, 2, or 18 km altitudes depending on the optical thickness of the gaseous absorber. Therefore, we can conclude that the reflected solar radiation measured in the O_2-A absorption band contains information about three to four parameters characterizing the vertical distribution of the aerosol particle number density. This conclusion agrees very well with results of extensive analyses of the information content of spectral measurements of the reflected solar radiation in the O_2-A absorption band with respect to the vertical distribution of aerosol optical properties reported in [20, 29].

6.7.2 Weighting functions for the cloud scattering coefficient

Let us further discuss WFs for the cloud scattering coefficient. As an example, we consider the reflected radiance at TOA in the O_2-A absorption band spectral range. Figure 6.5 shows vertical profiles of the scattering coefficient and the single scattering albedo within a water cloud located between 3 and 4 km altitude. The profiles are presented at two selected wavelengths for both vertically homogeneous and inhomogeneous water clouds. Here, the single scattering albedo of cloud, $\omega_c(z)$, is defined as follows:

$$\omega_c(z) = \frac{s_c(z)}{\sigma_e(z)}\,, \tag{6.107}$$

where $s_c(z)$ is the cloud scattering coefficient and $\sigma_e(z)$ is the extinction coefficient comprizing all absorption coefficients of atmospheric gases, Rayleigh scattering coefficient, and aerosol and cloud extinction coefficients. Therefore, the cloud single scattering albedo depends on the altitude even in the case of a vertically homogeneous cloud.

Now let us introduce the normalized weighting functions for cloud scattering coefficient, i.e., the weighting functions describing the relative variation of the intensity. Similarly to (6.102) we obtain for the relative variation of the intensity:

$$\frac{\Delta_i I(\tau_v, \Omega_v)}{I(\tau_v, \Omega_v)} = \frac{\mathcal{W}_{s_c}(\tau_i; \tau_v, \Omega_v)}{I(\tau_v, \Omega_v) s_c(\tau_i)} \Delta s_c(\tau_i) = \mathcal{R}_{s_c}(\tau_i; \tau_v, \Omega_v) \Delta s_c(\tau_i)\,. \tag{6.108}$$

Unlike the aerosol WFs, the normalized WFs, $\mathcal{R}_{s_c}(\tau_i; \tau_v, \Omega_v)$, introduced here describe the relative variation of the intensity caused by an absolute, $\Delta s_c(\tau_i)$, rather than a relative, $\Delta s_c(\tau_i)/s_c(\tau_i)$, variation of the cloud scattering coefficient. Thus, the introduced normalized WF, $\mathcal{R}_{s_c}(\tau_i; \tau_v, \Omega_v)$, is numerically equivalent to the relative variation of the intensity observed at the optical depth τ_v and

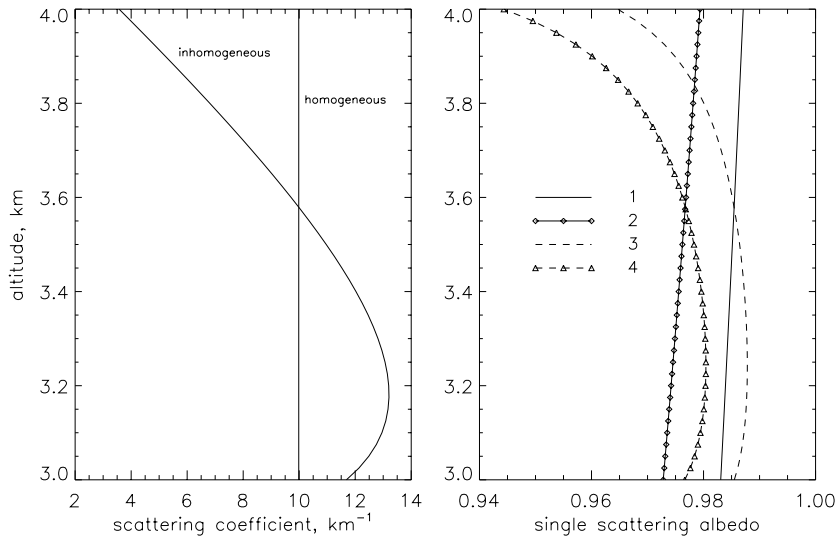

Fig. 6.5. Vertical profiles of the cloud scattering coefficient (left panel) and the cloud single scattering albedo (right panel) within a water cloud. The single scattering albedo is shown with solid lines (cases 1 and 2) for a homogeneous and with dashed lines (cases 3 and 4) for an inhomogeneous water cloud. The curves with and without symbols represent the single scattering albedo at 760.055 and 763.775 nm, respectively. The optical tickness of the gaseous absorbers at these wavelengths is 1.44 and 0.86, respectively.

direction Ω_v caused by $1\,\mathrm{km}^{-1}$ variation of the cloud scattering coefficient at the level τ_i.

Comparisons of the numerical and normalized layer-integrated analytical WFs for the cloud scattering coefficient at two selected wavelengths for a vertically homogeneous and inhomogeneous cloud are shown in Fig. 6.6 for the monochromatic case. The layer-integrated WFs were obtained according to (6.100) assuming the geometrical thickness of integration layers (i.e., $\tau_{i+1} - \tau_{i-1}$) to be 50 m. The numerical WFs were calculated employing the numerical perturbation approach assuming 0.01% variation of the cloud scattering coefficient. As can be seen from the plot an enhancement of the gaseous absorption inscreases maximum values of WFs. Although the altitudinal behavior of WFs in homogeneous and inhomogeneous clouds is similar, their maxima are located closer to the cloud top height in the case of a homogeneous cloud.

To illustrate the influence of the gaseous absorption on the WFs of the cloud scattering coefficient we consider the reflected radiation within the entire O_2-A absorption band. The spectral distribution of the reflected solar radiation observed at TOA in the nadir viewing geometry is shown in Fig. 6.7. The calculations were performed for a finite spectral resolution assuming the instrument slit function to be the boxcar function with a full width of 0.05 nm. To investigate the dependence of WFs on the optical thickness of gaseous absorbers we have selected five wavelengths marked in Fig. 6.7 by the numbers. The optical

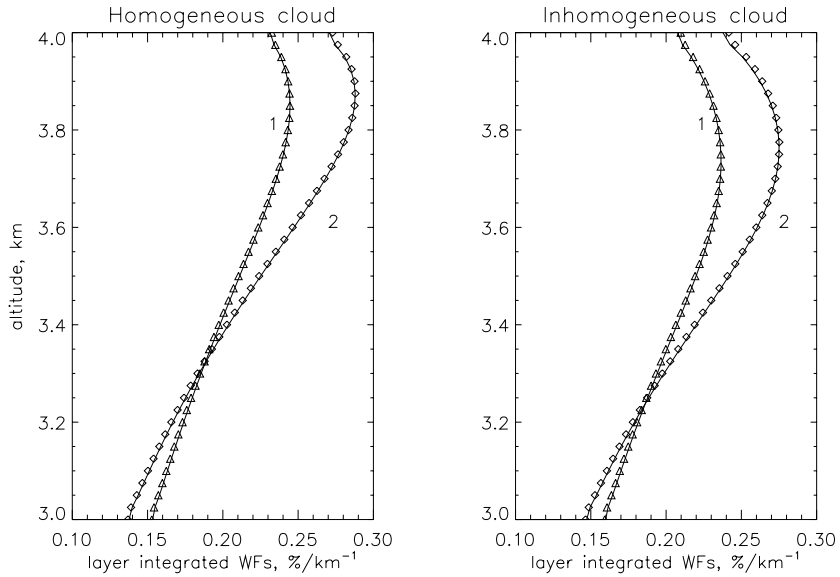

Fig. 6.6. Comparisons of the numerical (symbols) and normalized layer-integrated (solid line) WFs (layer geometrical thickness 50 m) for the cloud scattering coefficient at two selected wavelengths: 1, 763.775 nm ($\tau_g = 0.86$); 2, 760.055 nm ($\tau_g = 1.44$). The comparisons were performed for a solar zenith angle of 45°, surface albedo of 0.3, and cloud optical thickness of 10.

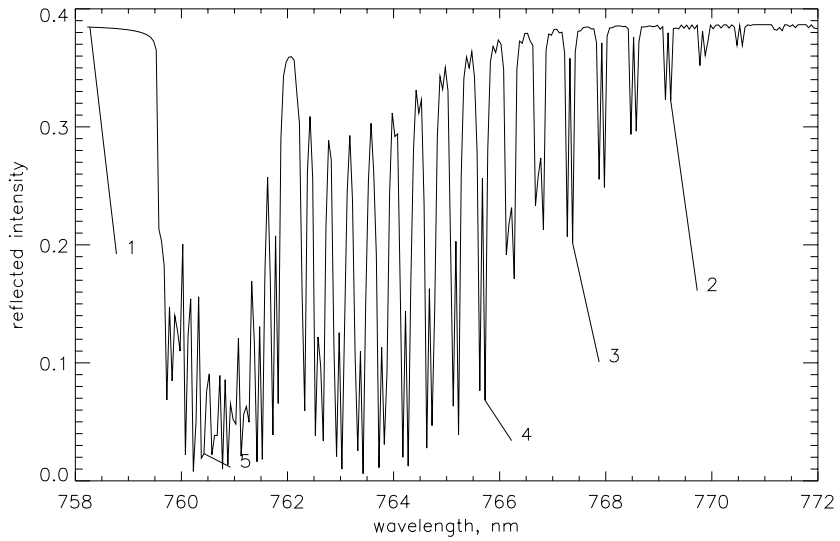

Fig. 6.7. Reflected solar radiation in the O_2-A absorption band spectral range in the presence of a homogeneous water cloud calculated for the same conditions as in Fig. 6.6. The wavelengths selected for presentation of the weighting functions in Fig. 6.8 are marked by the numbers.

thickness of gaseous absorbers ranges from 0.01 to 22 at these wavelengths. Figure 6.8 shows the normalized layer-integrated WFs at the selected wavelengths. At wavelengths where the gaseous absorption is weak, WFs are almost constant within the cloud demonstrating that no information on the vertical distribution of the cloud scattering coefficient within the cloud can be obtained. However, since the variation of the scattering coefficient at any altitude level within the cloud causes nearly the same variation of the reflected intensity, information on the optical thickness of the cloud independent of its vertical structure can be retrieved from measurements at these wavelengths. An enhancement in the optical thickness of the gaseous absorbers leads to an increased sensitivity of the reflected solar radiation to variations of the scattering coefficient in the upper part of a cloud. Thus, as can be seen from Fig. 6.8, for example, for the optical thickness of gaseous absorber of 9.11 a variation of the scattering coefficient of $1\,\mathrm{km}^{-1}$ near the cloud top height causes a variation of the intensity of about 0.24% whereas the same variation of the scattering coefficient near the cloud bottom results in just 0.15% variation of the intensity.

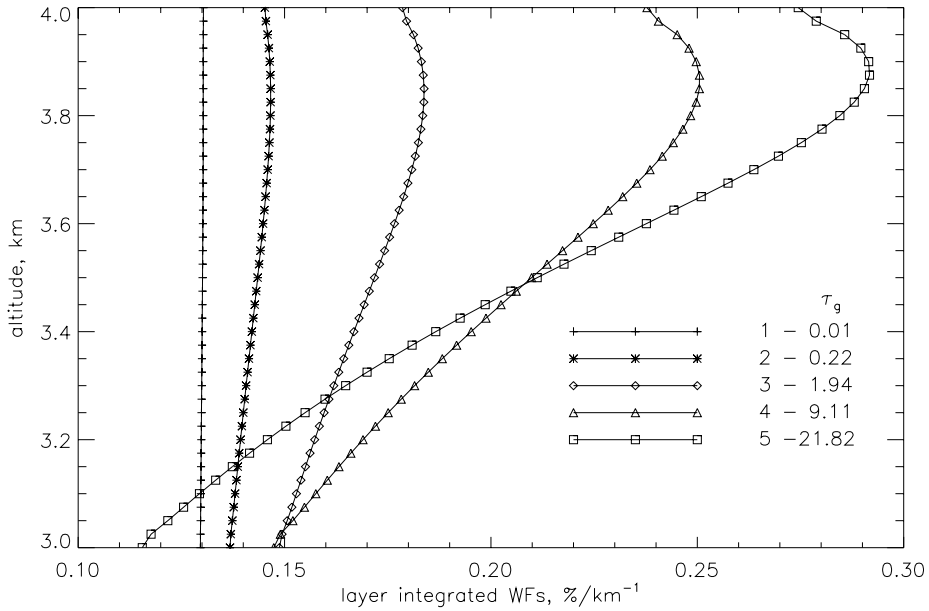

Fig. 6.8. Normalized layer-integrated WFs (layer geometrical thickness 50 m) for the cloud scattering coefficient at the wavelengths selected according to Fig. 6.7 corresponding to different values of optical thickness of gaseous absorber, τ_g.

6.8 Weighting functions for temperature and pressure

6.8.1 Theory

Variations in the vertical distributions of the temperature and pressure cause variations of the Rayleigh scattering coefficient as well as of the cross-sections of atmospheric gases. The strongest dependence on the temperature and pressure takes place in the near-infrared spectral range for the absorption cross-sections of atmospheric gases and in the ultraviolet spectral range for the Rayleigh scattering coefficient. In this section we will demonstrate that appropriate expressions for the temperature and pressure WFs can be obtained as a linear combination of WFs for the Rayleigh scattering coefficient and absorption coefficients of atmospheric gases employing the expressions for the scattering and absorption coefficients WFs derived in section 6.6. We will not consider here the variation of the Planck function caused by the variation in the vertical distributions of the temperature which is of great importance in the thermal spectral region only (see [30–32]).

Let us assume that the variation of the measured functional is caused by the variation of the gaseous absorption coefficient, $a_k(\tau)$, only. Then we can rewrite (6.6) as follows:

$$\delta\Phi(\tau_v, \Omega_v) = \int_0^{\tau_0} \mathcal{W}_{a_k}(\tau; \tau_v, \Omega_v) v_{a_k}(\tau)\, \mathrm{d}\tau\,, \tag{6.109}$$

where $\mathcal{W}_{a_k}(\tau; \tau_v, \Omega_v)$ given by (6.92) and $v_{a_k}(\tau)$ are the weighting function and the relative variation of the kth gaseous absorption coefficient, respectively. Assuming further that the concentration of the absorbing gas does not vary, we have

$$\delta a_k(\tau) = n_k(\tau)\delta\sigma_k(\tau)\,, \tag{6.110}$$

where $n_k(\tau)$ is the number density profile of kth absorbing gas and the variation of the absorption cross-section, $\delta\sigma_k(\tau)$, is caused by variations of the temperature and pressure. Employing the Taylor series expansion of the absorption cross-section as a function of the temperature, $T(\tau)$, and the pressure, $P(\tau)$, we obtain in the linear approximation:

$$\delta\sigma_k(\tau) = \frac{\partial\sigma_k(\tau)}{\partial T(\tau)}\delta T(\tau) + \frac{\partial\sigma_k(\tau)}{\partial P(\tau)}\delta P(\tau)\,, \tag{6.111}$$

where $\partial\sigma_k(\tau)/\partial T(\tau)$ and $\partial\sigma_k(\tau)/\partial P(\tau)$ are the partial derivatives of the cross-section with respect to temperature and pressure, respectively. The partial derivatives can be calculated analytically or numerically. Substituting $\delta a_k(\tau)$ given by (6.110) into (6.109) and taking into account (6.111), we obtain the following linear relationship between the variation of the measured functional and variations of $T(\tau)$ and $P(\tau)$:

$$\delta\Phi(\tau_v, \Omega_v) = \int_0^{\tau_0} \frac{\mathcal{W}_{a_k}(\tau; \tau_v, \Omega_v)}{\sigma_k(\tau)} \left[\frac{\partial\sigma_k(\tau)}{\partial T(\tau)}\delta T(\tau) + \frac{\partial\sigma_k(\tau)}{\partial P(\tau)}\delta P(\tau)\right] \mathrm{d}\tau\,. \tag{6.112}$$

Thus, WFs for the temperature and pressure profiles are obtained as follows:

$$\mathcal{W}_T^a(\tau;\tau_v,\Omega_v) = \sum_{k=1}^{K} \frac{\partial \ln \sigma_k(\tau)}{\partial T(\tau)} \mathcal{W}_{a_k}(\tau;\tau_v,\Omega_v)\,, \tag{6.113}$$

$$\mathcal{W}_P^a(\tau;\tau_v,\Omega_v) = \sum_{k=1}^{K} \frac{\partial \ln \sigma_k(\tau)}{\partial P(\tau)} \mathcal{W}_{a_k}(\tau;\tau_v,\Omega_v)\,, \tag{6.114}$$

where K is the full number of absorbing atmospheric gases. The superscript 'a' is introduced to emphasize that the corresponding WFs describe the variation of the measured functional caused by variations of the gaseous absorption coefficients.

In the ultraviolet and visible spectral ranges the variations of the temperature and pressure cause not only variations of the absorption cross-sections but also the variation of the Rayleigh scattering coefficient which is strongly dependent on the air number density and, therefore, on the temperature and pressure. To account for the contribution of the Rayleigh scattering coefficient variation into the variation of the measured functional we rewrite (6.109) in the following form:

$$\delta\Phi(\tau_v,\Omega_v) = \int_0^{\tau_0} \mathcal{W}_{s_k}(\tau;\tau_v,\Omega_v) v_{s_k}(\tau)\,\mathrm{d}\tau\,, \tag{6.115}$$

where we have assumed that the variation of the measured functional is caused only by the variation of the Rayleigh scattering coefficient whose relative variation is represented by $v_{s_k}(\tau)$. Employing the Taylor series expansion of the Rayleigh scattering coefficient as a function of the temperature and pressure, we obtain in the linear approximation:

$$\delta s_k(\tau) = \frac{\partial s_k(\tau)}{\partial T(\tau)} \delta T(\tau) + \frac{\partial s_k(\tau)}{\partial P(\tau)} \delta P(\tau)\,. \tag{6.116}$$

Similarly to (6.113) and (6.114) the contribution of the Rayleigh scattering coefficient to the temperature and pressure WFs can be obtained as follows:

$$\mathcal{W}_T^r(\tau;\tau_v,\Omega_v) = \frac{\partial \ln s_k(\tau)}{\partial T(\tau)} \mathcal{W}_{s_k}(\tau;\tau_v,\Omega_v)\,, \tag{6.117}$$

$$\mathcal{W}_P^r(\tau;\tau_v,\Omega_v) = \frac{\partial \ln s_k(\tau)}{\partial P(\tau)} \mathcal{W}_{s_k}(\tau;\tau_v,\Omega_v)\,. \tag{6.118}$$

Here, the superscript 'r' is introduced to emphasize that the corresponding WFs describe the variation of the measured functional caused by the variation of the Rayleigh scattering coefficient.

Thus, accounting for contributions of both the gaseous absorption and the Rayleigh scattering, the temperature and pressure WFs are obtained as

$$\mathcal{W}_T(\tau;\tau_v,\Omega_v) = \mathcal{W}_T^a(\tau;\tau_v,\Omega_v) + \mathcal{W}_T^r(\tau;\tau_v,\Omega_v)\,, \tag{6.119}$$

$$\mathcal{W}_P(\tau;\tau_v,\Omega_v) = \mathcal{W}_P^a(\tau;\tau_v,\Omega_v) + \mathcal{W}_P^r(\tau;\tau_v,\Omega_v)\,. \tag{6.120}$$

Derived WFs describe the contribution of variations of the temperature and pressure at a given optical depth into the variation of the measured functional. Assuming that the absolute variation of the temperature and the relative variation of the pressure can be considered to be independent of the altitude, the integrated WFs can be introduced as follows:

$$\mathcal{W}_T(\tau_v, \Omega_v) = \int_0^{\tau_0} \mathcal{W}_T(\tau; \tau_v, \Omega_v)\, \mathrm{d}\tau\,, \tag{6.121}$$

$$\mathcal{W}_P(\tau_v, \Omega_v) = \int_0^{\tau_0} \mathcal{W}_P(\tau; \tau_v, \Omega_v) P(\tau)\, \mathrm{d}\tau\,. \tag{6.122}$$

6.8.2 Examples

Using the integrated WFs, the variation of the measured functional can be rewritten in the following form:

$$\delta\Phi(\tau_v, \Omega_v) = \mathcal{W}_T(\tau_v, \Omega_v)\Delta T + \mathcal{W}_P(\tau_v, \Omega_v)\frac{\Delta P}{P}\,, \tag{6.123}$$

where ΔT and $\Delta P/P$ are the absolute variation of the temperature and the relative variation of the pressure, respectively, considered to be constant in the entire atmosphere. Dividing both sides of (6.123) by the measured functional, we introduce the normalized WFs for the temperature and pressure as follows:

$$\frac{\delta\Phi(\tau_v, \Omega_v)}{\Phi(\tau_v, \Omega_v)} = \mathcal{R}_T(\tau_v, \Omega_v)\Delta T + \mathcal{R}_P(\tau_v, \Omega_v)\frac{\Delta P}{P}\,, \tag{6.124}$$

where

$$\mathcal{R}_T(\tau_v, \Omega_v) = \frac{\mathcal{W}_T(\tau_v, \Omega_v)}{\Phi(\tau_v, \Omega_v)}\,,\ \mathcal{R}_P(\tau_v, \Omega_v) = \frac{\mathcal{W}_P(\tau_v, \Omega_v)}{\Phi(\tau_v, \Omega_v)}\,. \tag{6.125}$$

Spectral dependence of $\mathcal{R}_T(\tau_v, \Omega_v)$ and $\mathcal{R}_P(\tau_v, \Omega_v)$ functions appropriate to observations of the reflected solar radiance in the nadir viewing geometry is illustrated in Fig. 6.9 for the CO_2 absorption band spectral range, where only the gaseous absorption is substantial, and in Fig. 6.10 for 320–330 nm spectral range, where contributions of both the Rayleigh scattering and the ozone absorption are significant. The numerical WFs for the temperature and pressure shown in Figs 6.9 and 6.10 were calculated using the numerical perturbation approach according to (6.98) assuming a relative variation of the pressure of 0.01% and an absolute variation of the temperature of 0.1 K at each atmospheric level. As can be seen from Fig. 6.9 the variation of the reflected intensity within the CO_2 absorption band ranges from 0% to about −0.055% then caused by 1% variation of the pressure and from −0.055% to about 0.045% then caused by 1K variation in the temperature. Moreover, spectral dependencies of these variations are very different. Contributions of other gaseous absorbers as well as of the Rayleigh

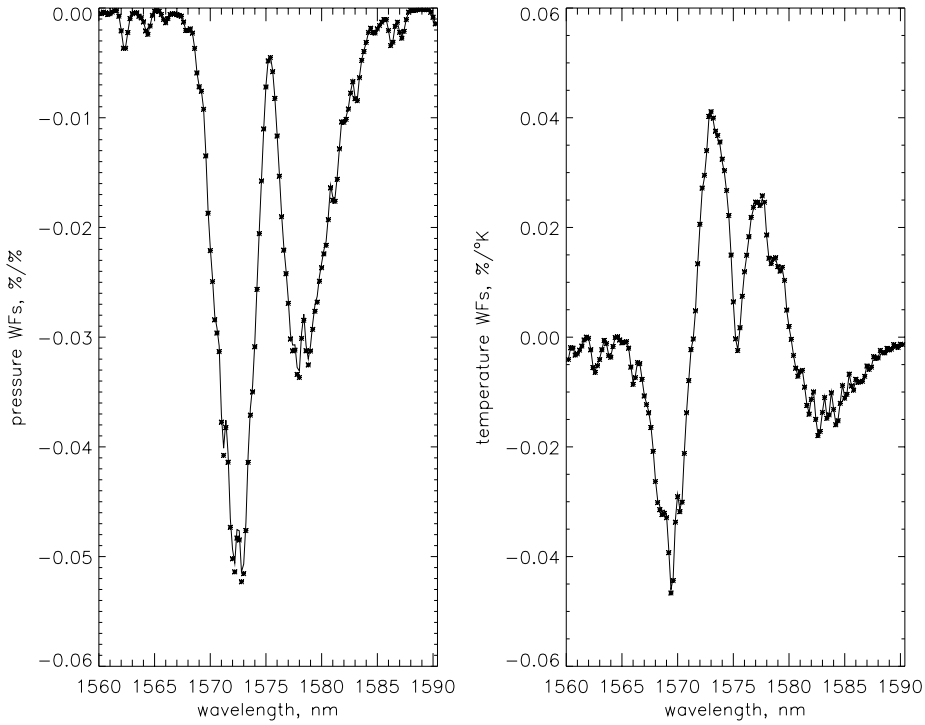

Fig. 6.9. Numerical (symbols) and normalized integrated analytical (solid line) WFs for relative variations of the pressure (left panel) and absolute variations of the temperature (right panel). Calculations were performed for the reflected intensity observed at TOA in the nadir viewing geometry at a solar zenith angle of 40°. The surface albedo was set to zero.

scattering can be neglected in this spectral range. This is, however, not the case in 320–330 nm spectral range shown in Fig. 6.10. Here, due to the strong contribution of the Rayleigh scattering, the relative variations of the intensity are about an order of magnitude larger than in the CO_2 absorption band spectral range. For example, 1% variation of the pressure causes 0.7% variation of the reflected intensity, whereas 1 K variation in the temperature results in −0.35% variation of the intensity.

Even if the relative variations of the reflected intensity cased by variations of atmospheric trace gas cross-sections are quite small, as occurs in the CO_2 absorption band spectral range shown in Fig. 6.9, they can result in noticeable additional errors in the retrieved trace gas number densities if corresponding parameters are neglected. For known uncertainties in the pressure and temperature these errors can be estimated employing the obtained WFs.

Relative variations of the reflected intensity in CO_2 absorption band spectral range due to 1% variation of CO_2 number density, 1% variation of the pressure, and 1 K variation of the temperature are shown in Fig. 6.11. We note that relative

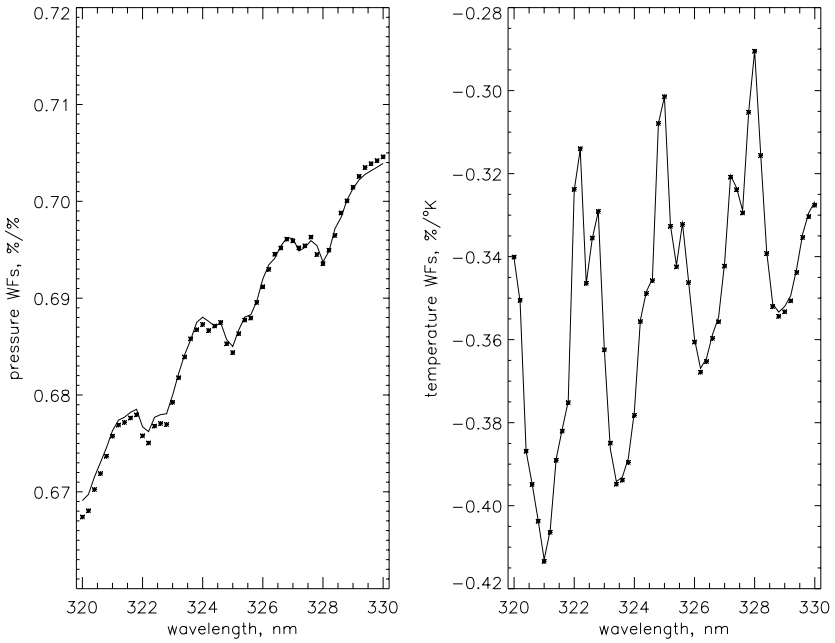

Fig. 6.10. Same as Fig. 6.9 but for 320–330 nm spectral range.

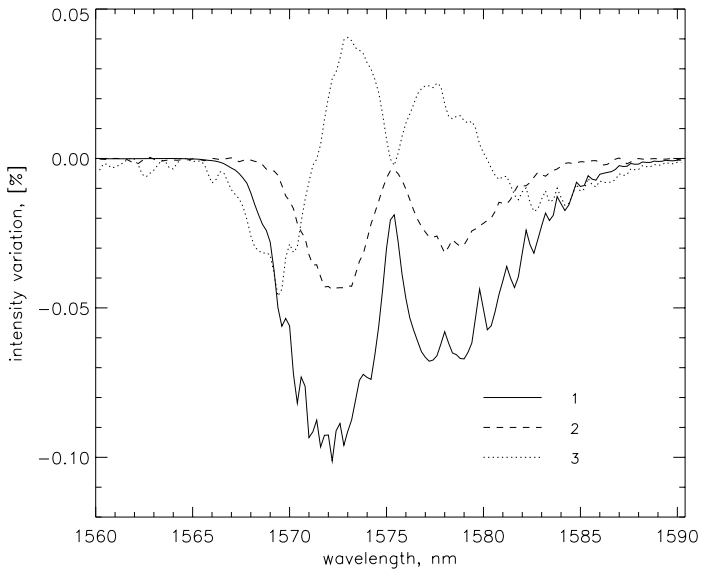

Fig. 6.11. Relative variations of the reflected intensity in CO_2 absorption band spectral range due to 1% variation of CO_2 number density (1), 1% variation of the pressure (2), and 1K variation of the temperature (3). Calculations were performed for the reflected intensity observed at TOA in the nadir viewing geometry at a solar zenith angle of 40°. The surface albedo was set to zero.

variations of the absorber number density and of the corresponding absorption coefficient result in the same relative variation of the reflected intensity (see [24] for details). As can be seen from Fig. 6.11, the relative variations of the observed intensity due to variations of the pressure and CO_2 number density have very similar spectral dependence, whereas the response to 1% variation of CO_2 number density is by a factor ∼2.5 stronger as compared to 1% variation of the pressure. Thus, this simple comparison allows us to conclude that 1% retrieval accuracy for CO_2 number density can only be achieved if the uncertainty of the atmospheric pressure does not exceed 2.5%. In the same manner, the influence of the temperature and other atmospheric parameters on the retrieval accuracy of CO_2 number density can be evaluated as well. Essential results of a quantitative analysis using the weighting function approach in the considered spectral range are reported in [3].

6.9 Weighting functions for particle number concentration and effective radius of droplets

6.9.1 Cloud parameters

The main optical parameters of a cloud are the scattering coefficient, the absorption coefficient, and the phase function. In the case of a vertically inhomogeneous cloud these parameters are usually defined within the cloud as functions of the altitude. Taking into account that the same cloud can be located at different altitudes in the atmosphere, it is more convenient to employ a dimensionless variable to describe vertical profiles of cloud parameters. As such a variable we introduce

$$x = \frac{z_t - z}{z_t - z_b}\,, \tag{6.126}$$

where z_t and z_b are the cloud top height (CTH) and cloud bottom height (CBH), respectively. The variable x is dimensionless and ranges from 0 at CTH to 1 at CBH. The vertical profiles of cloud optical parameters can be defined using two different approaches. The first one is to define the shape of the cloud extinction coefficient, $s_h(x)$, within the cloud as a function of the dimensionless variable x. Then assuming the water droplet or ice crystal single scattering albedo, ω_k, to be constant within the cloud, we obtain the following expressions for the cloud scattering, $s_k(z)$, and absorption, $a_k(z)$, coefficients:

$$s_k(z) = c\ \omega_k s_h(z)\,, \tag{6.127}$$

$$a_k(z) = c\ (1 - \omega_k) s_h(z)\,, \tag{6.128}$$

where c is the scaling parameter obtained requiring the optical thickness of the cloud to be equal a pre-defined value of the optical thickness, τ_c, which is considered to be an input optical integral parameter. Introducing the optical thickness, τ_{s_h}, corresponding to the shape of the extinction coefficient, $s_h(z)$, as follows:

$$\tau_{s_h} = \int_{z_b}^{z_t} s_h(z)\,\mathrm{d}z\,, \tag{6.129}$$

we obtain for the scaling factor:

$$c = \frac{\tau_c}{\tau_{s_h}}\,. \tag{6.130}$$

Thus, according to this approach the input parameters for the cloud are: single scattering albedo, cloud optical thickness, and shape of the extinction coefficient. The phase function is assumed to be constant within the cloud. This approach will be used to define optical characteristics of water or ice clouds.

The second approach is based on the parameterization of the local optical characteristics of the cloud such as the extinction coefficient and the single scattering albedo. The extinction coefficients of water droplets, $e_1(z)$, and ice crystals, $e_2(z)$, can be represented in the form of the following analytical expressions [8]:

$$e_1(z) = \frac{3l_1(z)}{2r_1(z)\rho_1}K_e(z)\,, \tag{6.131}$$

$$K_e(z) = 1 + Ax_1^{-2/3}(z) - B\left[1 - e^{Cx_1^{-2/3}(z)}\right]\,, \tag{6.132}$$

$$e_2(z) = \frac{3l_2(z)}{2r_2(z)\rho_2}\,, \tag{6.133}$$

where subscripts '1' and '2' correspond to water droplets and ice crystals, respectively; $l_1(z)$ and $l_2(z)$ are the liquid water content (LWC) and ice water content (IWC), respectively; $r_1(z)$ and $r_2(z)$ are the effective radii of particles defined as

$$r_k(z) = \frac{3\bar{V}_k(z)}{\bar{G}_k(z)}\,, \quad k = 1, 2\,, \tag{6.134}$$

where $\bar{V}_k(z)$ and $\bar{G}_k(z)$ are the average volume and the average surface area of particles, respectively; $x_k(z) = 2\pi r_k(z)/\lambda$; λ is the wavelength; ρ_1 and ρ_2 are the densities of the water and ice, respectively. Constants A, B, and C are calculated employing the Mie theory: $A = 1.1$, $B = 1.7\ 10^{-6}$ and $C = 56.3$ [8].

The absorption properties of the water and ice particles are defined by the parameterization of the water droplets absorption coefficient, $a_1(z)$, and ice crystals single scattering albedo, $\omega_2(z)$, as follows [8]:

$$a_1(z) = \frac{4\pi\chi_1}{\lambda\rho_1}l_1(z)K_a(z)\,, \tag{6.135}$$

$$K_a(z) = 1.23\Big[1 - 2.6x_1(z)\chi_1\Big]\Big[1 + 0.34\left(1 - \mathrm{e}^{-8\lambda/r_1(z)}\right)\Big]\,, \tag{6.136}$$

$$\omega_2(z) = 1 - 0.47K_\omega(z)\,, \tag{6.137}$$

$$K_\omega(z) = 1 - e^{-2\eta x_2(z)\chi_2}\,. \tag{6.138}$$

Here, χ_k represents the imaginary part of the refractive index $m_k = n_k - i\chi_k$ of water ($k = 1$) and ice ($k = 2$), the parameter η depends on the assumed shape of ice crystals. It is equal to 3.6 for fractal particles used in this work.

Summing up all obtained results, the scattering coefficient of the cloud will be defined as

$$s_1(z) = \frac{l_1(z)}{\rho_1}\left[\frac{3K_e(z)}{2r_1(z)} - \frac{4\pi\chi_1}{\lambda}K_a(z)\right], \tag{6.139}$$

$$s_2(z) = \frac{3}{2}\frac{l_2(z)}{r_2(z)\rho_2}\left[1 - 0.47K_\omega(z)\right], \tag{6.140}$$

and the absorption coefficient as

$$a_1(z) = \frac{l_1(z)}{\rho_1}\frac{4\pi\chi_1}{\lambda}K_a(z), \tag{6.141}$$

$$a_2(z) = \frac{3}{2}\frac{l_2(z)}{r_2(z)\rho_2}0.47K_\omega(z). \tag{6.142}$$

Thus, according to the second approach the input parameters for the cloud are:

- the vertical profiles of the liquid water and/or ice content;
- the vertical profiles of the effective radius of water droplets and/or ice crystals;
- the imaginary part of the refractive index for water and/or ice.

The phase function is assumed to be constant within the cloud. This approach will be used to define the local optical properties of water, ice or mixed clouds.

The accuracy of the proposed approximations has been studied in [8]. Comparisons of the obtained approximative formulae to the results of exact calculations show that the relative errors of the extinction coefficient approximation are below 1% for $\lambda < 2.5\,\mu$m and effective radii of water droplets greater than $4\,\mu$m. The accuracy of the approximative expression for the absorption coefficient is better than 10% for $\lambda < 2.5\,\mu$m and the effective radii of water droplets between 4 and $16\,\mu$m. In the spectral range, where the absorption of the liquid water is weaker ($\lambda < 1.8\,\mu$m), the accuracy of the absorption coefficient approximation is better than 5% for the same range of the effective radius.

The integral properties of the cloud such as cloud optical thickness (COT), liquid water path (LWP), and ice water path (IWP) are obtained as follows:

$$\tau_{c_k} = \int_{z_b}^{z_t} e_k(z)\,\mathrm{d}z\,,\ k = 1, 2\,, \tag{6.143}$$

$$LWP = \int_{z_b}^{z_t} l_1(z)\,\mathrm{d}z\,, \quad IWP = \int_{z_b}^{z_t} l_2(z)\,\mathrm{d}z\,, \tag{6.144}$$

where $e_k(z)$ is the extinction coefficient of water ($k = 1$) or ice ($k = 2$). Thus, according to this approach, COT, LWP, and IWP are not considered as input parameters.

In the parameterization of the local cloud optical parameters given by (6.139)–(6.142) the liquid or ice water content and effective radius are considered as two independent variables. However, at least for a water cloud, there is a known relationship between LWC and the radius of water droplets. Assuming that the size distribution of water droplets is given by the function $f(r, z)$ normalized as follows:

$$\int_0^\infty f(r, z)\,\mathrm{d}r = 1\,, \tag{6.145}$$

where r is the radius of water droplets, LWC at a given altitude z can be expressed as

$$l_1(z) = \frac{4\pi\rho_1}{3} N(z) \int_0^\infty r^3 f(r, z)\,\mathrm{d}r\,, \tag{6.146}$$

where ρ_1 is the density of the liquid water and $N(z)$ is the particle number concentration of droplets. Introducing the third moment of the size distribution function as follows:

$$\langle r^3(z)\rangle = \int_0^\infty r^3 f(r, z)\,\mathrm{d}r \tag{6.147}$$

and substituting it into (6.146), we obtain

$$l_1(z) = \frac{4\pi\rho_1}{3} N(z)\langle r^3(z)\rangle\,. \tag{6.148}$$

In most cases, the measured particle size distribution function, $f(r, z)$, can be approximated by the gamma distribution (see [7] and references therein):

$$f(r, z) = B r^\mu\, \mathrm{e}^{-\mu[r/r_0(z)]}\,, \tag{6.149}$$

where,

$$B = \frac{\mu^{\mu+1}}{\Gamma(\mu+1) r_0^{\mu+1}(z)} \tag{6.150}$$

is the normalization constant and $\Gamma(\mu+1)$ is the gamma function. The parameters μ and $r_0(z)$ characterize the width and the maximum position of the particle size distribution function, respectively. Now let us assume that only parameter $r_0(z)$ depends on the altitude z. In this case the following expressions for $\langle r^3(z)\rangle$ and the effective radius, $r_1(z)$, can be obtained:

$$\langle r^3(z)\rangle = \left(\frac{r_0(z)}{\mu}\right)^3 \frac{\Gamma(4+\mu)}{\Gamma(1+\mu)}\,, \tag{6.151}$$

$$r_1(z) = \frac{r_0(z)}{\mu}\,(3+\mu)\,. \tag{6.152}$$

Taking into account properties of the gamma function [13], we obtain the following relationship between the third moment and the effective radius:

$$\langle r^3(z)\rangle = r_1^3(z)\frac{(\mu+2)(\mu+1)}{(\mu+3)^2}\,. \tag{6.153}$$

Substituting obtained expression into (6.148) it follows:

$$l_1(z) = \frac{4\pi\rho_1}{3}\frac{(\mu+2)(\mu+1)}{(\mu+3)^2}N(z)r_1^3(z)\,. \tag{6.154}$$

Thus, for a water cloud, instead of the parameterization via dependent parameters $l_1(z)$ and $r_1(z)$ we have obtained parameterization via an independent pair $N(z)$ and $r_1(z)$. This relationship is often used by the retrieval of water-cloud droplet effective radius (see [5] and references therein).

6.9.2 Weighting functions

In this subsection we derive the weighting functions for the particle number concentration, $N(z)$, liquid water content, $l_1(z)$, and the effective radius of water droplets, $r_1(z)$. We start from expressions for the weighting functions for the cloud absorption and scattering coefficients given by (6.92) and (6.97), respectively. Let us assume that the variation of the measured functional, $\delta\Phi$, is caused by the variation of the cloud scattering, $s_1(\tau)$, and absorption, $a_1(\tau)$, coefficients of the water droplets only. Then according to (6.68) we have

$$\delta\Phi(\tau_v,\Omega_v) = \int_0^{\tau_0}\left[\mathcal{W}_{s_1}(\tau;\tau_v,\Omega_v)v_{s_1}(\tau) + \mathcal{W}_{a_1}(\tau;\tau_v,\Omega_v)v_{a_1}(\tau)\right]\mathrm{d}\tau\,, \tag{6.155}$$

where $v_{s_1}(\tau) = \delta s_1(\tau)/s_1(\tau)$ and $v_{a_1}(\tau) = \delta a_1(\tau)/a_1(\tau)$ are the relative variations of the scattering and absorption coefficients of water droplets, respectively. The variation of the scattering and absorption coefficients given by (6.139) and (6.141), respectively, can be caused by the variations of the particle number concentration and the effective radius. Varying the expression for the scattering coefficient given by (6.139) with respect to $N(z)$ and $r_1(z)$, we obtain

$$\delta s_1(z) \;=\; F_s(z)\frac{\partial l_1(z)}{\partial N(z)}\delta N(z) + \left[F_s(z)\frac{\partial l_1(z)}{\partial r_1(z)} + l_1(z)\frac{\partial F_s(z)}{\partial r_1(z)}\right]\delta r_1(z)\,, \tag{6.156}$$

where the function $F_s(z)$ is defined as follows:

$$F_s(z) = \frac{1}{\rho_1}\left[\frac{3}{2}\frac{K_e(z)}{r_1(z)} - \frac{4\pi\chi_1}{\lambda}K_a(z)\right]\,. \tag{6.157}$$

Equation (6.156) was obtained taking into account that according to (6.154) the liquid water content is a function of $N(z)$ and $r_1(z)$. If we consider the liquid water content as an independent variable, then varying the expression for the scattering coefficient given by (6.139) with respect to $l_1(z)$ and $r_1(z)$, we obtain

$$\delta s_1(z) \;=\; F_s(z)\delta l_1(z) + l_1(z)\frac{\partial F_s(z)}{\partial r_1(z)}\delta r_1(z)\,. \tag{6.158}$$

Taking into account that $\partial l_1(z)/\partial N(z) = l_1(z)/N(z)$ and $\partial l_1(z)/\partial r_1(z) = 3l_1(z)/r_1(z)$ as well as $F_s(z) = s_1(z)/l_1(z)$, we rewrite (6.156) and (6.158) in the following form:

$$\delta s_1(z) = s_1(z)\frac{\delta N(z)}{N(z)} + 3s_1(z)\frac{\delta r_1(z)}{r_1(z)} + l_1(z)\frac{\partial F_s(z)}{\partial r_1(z)}\delta r_1(z)\,. \quad (6.159)$$

$$\delta s_1(z) = s_1(z)\frac{\delta l_1(z)}{l_1(z)} + l_1(z)\frac{\partial F_s(z)}{\partial r_1(z)}\delta r_1(z)\,. \quad (6.160)$$

Dividing both sides of this equation by $s_1(z)$, the relative variation of the scattering coefficient can now be obtained via the variation of the particle number concentration or of the liquid water content and of the effective radius of water droplets as follows:

$$v_{s_1}(z) = v_N(z) + \left(3 + \frac{r_1(z)}{F_s(z)}\frac{\partial F_s(z)}{\partial r_1(z)}\right) v_r(z)\,, \quad (6.161)$$

$$v_{s_1}(z) = v_{l_1}(z) + \frac{r_1(z)}{F_s(z)}\frac{\partial F_s(z)}{\partial r_1(z)} v_r(z)\,, \quad (6.162)$$

where $v_N(z)$, $v_{l_1}(z)$, and $v_r(z)$ are the relative variations of the particle number concentration, liquid water content and the effective radius, respectively. Taking into account that

$$\frac{r_1(z)}{F_s(z)}\frac{\partial F_s(z)}{\partial r_1(z)} = \frac{\partial \ln F_s(z)}{\partial \ln r_1(z)}\,, \quad (6.163)$$

Equations (6.161) and (6.162) can be rewritten as follows:

$$v_{s_1}(z) = v_N(z) + \left(3 + \frac{\partial \ln F_s(z)}{\partial \ln r_1(z)}\right) v_r(z)\,, \quad (6.164)$$

$$v_{s_1}(z) = v_{l_1}(z) + \frac{\partial \ln F_s(z)}{\partial \ln r_1(z)} v_r(z)\,. \quad (6.165)$$

The expression for the variation of the absorption coefficient, $\delta a_1(z)$, can be derived in a way analogous to the derivation of $\delta s_1(z)$. Introducing the function $F_a(z)$ as follows:

$$F_a(z) = \frac{4\pi\chi_1}{\lambda\rho_1} K_a(z)\,, \quad (6.166)$$

we obtain

$$v_{a_1}(z) = v_N(z) + \left(3 + \frac{\partial \ln F_a(z)}{\partial \ln r_1(z)}\right) v_r(z)\,, \quad (6.167)$$

$$v_{a_1}(z) = v_{l_1}(z) + \frac{\partial \ln F_a(z)}{\partial \ln r_1(z)} v_r(z)\,. \quad (6.168)$$

The weighting functions for relative variations of the particle number concentration and effective radius of water droplets can now be obtained substituting $v_{s_1}(z)$, and $v_{a_1}(z)$ given by (6.164) and (6.167), respectively, into (6.155):

$$\mathcal{W}_N(\tau;\tau_v,\Omega_v) = \mathcal{W}_{s_1}(\tau;\tau_v,\Omega_v) + \mathcal{W}_{a_1}(\tau;\tau_v,\Omega_v)\,, \tag{6.169}$$

$$\mathcal{W}_r^N(\tau;\tau_v,\Omega_v) = \tilde{F}_s(z)\mathcal{W}_{s_1}(\tau;\tau_v,\Omega_v) + \tilde{F}_a(z)\mathcal{W}_{a_1}(\tau;\tau_v,\Omega_v)\,, \tag{6.170}$$

where

$$\tilde{F}_s(z) = 3 + \frac{\partial \ln F_s(z)}{\partial \ln r_1(z)}\,, \quad \tilde{F}_a(z) = 3 + \frac{\partial \ln F_a(z)}{\partial \ln r_1(z)}\,, \tag{6.171}$$

and the superscript 'N' of the WF for the effective radius denotes that this weighting function corresponds to the pair (N,r), i.e., the particle number concentration and effective radius are considered as independent parameters.

The weighting functions for relative variations of the liquid water content and effective radius of water droplets can be obtained in an analogous way substituting $v_{s_1}(z)$, and $v_{a_1}(z)$ given by (6.165) and (6.168), respectively, into (6.155):

$$\mathcal{W}_{l_1}(\tau;\tau_v,\Omega_v) = \mathcal{W}_{s_1}(\tau;\tau_v,\Omega_v) + \mathcal{W}_{a_1}(\tau;\tau_v,\Omega_v)\,, \tag{6.172}$$

$$\mathcal{W}_r^{LWC}(\tau;\tau_v,\Omega_v) = \frac{\partial \ln F_s(z)}{\partial \ln r_1(z)}\mathcal{W}_{s_1}(\tau;\tau_v,\Omega_v) + \frac{\partial \ln F_a(z)}{\partial \ln r_1(z)}\mathcal{W}_{a_1}(\tau;\tau_v,\Omega_v)\,, \tag{6.173}$$

where the superscript 'LWC' of the WF for the effective radius denotes that this weighting function corresponds to the pair (LWC,r). Comparing expressions for WFs obtained for the pairs (N,r) and (LWC,r), we see that WFs for the relative variation of the particle number concentration and the relative variation of the liquid water content are identical. The relationship between $\mathcal{W}_r^{LWC}$ and $\mathcal{W}_r^N$ obtained for pairs (LWC,r) and (N,r), respectively, can be easily derived:

$$\mathcal{W}_r^N(\tau;\tau_v,\Omega_v) = \mathcal{W}_r^{LWC}(\tau;\tau_v,\Omega_v) + 3\,\mathcal{W}_N(\tau;\tau_v,\Omega_v)\,. \tag{6.174}$$

Therefore, we obtain the linear relationship between the variation of the measured functional, $\delta\Phi(\tau_v,\Omega_v)$, and relative variations of the particle number concentration and effective radius of water droplets as follows:

$$\delta\Phi(\tau_v,\Omega_v) = \int_0^{\tau_0} \left[\mathcal{W}_N(\tau;\tau_v,\Omega_v)v_N(\tau) + \mathcal{W}_r^N(\tau;\tau_v,\Omega_v)v_r(\tau)\right] \mathrm{d}\tau\,. \tag{6.175}$$

Introducing as a vertical coordinate the altitude z instead of the optical depth, τ, and taking into account that variations of cloud parameters are non-zero only within the cloud, we can rewrite (6.175) in the following form:

$$\delta\Phi(z_v,\Omega_v) = \int_{z_b}^{z_t} \left[\mathcal{W}_N(z;z_v,\Omega_v)v_N(z) + \mathcal{W}_r^N(z;z_v,\Omega_v)v_r(z)\right] \sigma_e(z)\,\mathrm{d}z\,. \tag{6.176}$$

This equation can be used to retrieve vertical profiles of the particle number concentration and the effective radius of water droplets from measurements of the transmitted or reflected solar radiation in the range of the liquid water absorption or both within and outside the absorption bands of gaseous components such as O_2, O_4, or CO_2.

6.10 Examples of weighting functions for particle number concentration, liquid water content, and effective radius of water droplets

In this section we consider selected examples of WFs for the particle number concentration, liquid water content and effective radius of water droplets calculated using expressions obtained in the previous section. The normalized layer-integrated WFs for relative variations of the effective radius of water droplets and the liquid water content corresponding to the pair (LWC,r) are shown in Fig. 6.12 at four selected wavelengths. All calculations were performed for a vertically homogeneous water cloud having an optical thickness of 10. The wavelengths were selected as follows: one spectral point within the O_2-A absorption band characterized by a strong gaseous absorption (760.425 nm), two spectral points within absorption bands of the liquid water (1.6 μm and 2.2 μm), and one point in a spectral range where no absorption features are present (758.2 nm). WFs shown here are defined as:

$$\mathcal{R}_p(\tau_i;\tau_v,\Omega_v) = \frac{\mathcal{W}_p(\tau_i;\tau_v,\Omega_v)}{I(\tau_v,\Omega_v)}\,, \tag{6.177}$$

where subscript p is equal to 'r' or to 'l_1' for the effective radius of water droplets and LWC, respectively. The function $\mathcal{R}_p(\tau_i;\tau_v,\Omega_v)$ equals to the percentage variation of the reflected intensity observed at TOA in the nadir viewing geometry caused by a 1% variation of corresponding parameters at a given position within a layer of 50 m geometrical thickness.

As can be seen from Fig. 6.12, WFs for LWC are always positive whereas WFs for the effective radius of water droplets are always negative. This can be easily explained considering the analytical expression for the water cloud scattering coefficient given by (6.139). Indeed, the scattering coefficient is proportional to LWC and inversely proportional to the effective radius of water droplets. Therefore, an enhancement of the liquid water content leads to an enhancement of the scattering coefficient and, thus, of the cloud optical thickness which results, in turn, in an increase in the reflected intensity. This is why WFs for the liquid water content are positive. These WFs show very week dependence on the altitude at all considered wavelengths with exception of the spectral point at a strong gaseous absorption (760.425 nm) where the sensitivity of the reflected radiation to the variation of LWC near the cloud top is as large as twice the sensitivity to the variation in the bottom cloud layers. Unlike LWC weighting functions, WFs for the effective radius of water droplets show a significant dependence on the altitude for all wavelengths where the gaseous or liquid water absorption occurs whereas there is absolutely no altitude dependence of WF at spectral points where no absorption signatures are present (758.2 nm). The maxima of WFs are located near the cloud top. For example, as seen from the left panel in Fig. 6.12, WF for the effective radius of water droplets at 2.2 μm wavelength in the layers near the cloud top height is as large as twice the WF in the bottom cloud layers.

In the previous section we have derived the expression for the effective radius WF introducing as an independent variable the particle number concentration

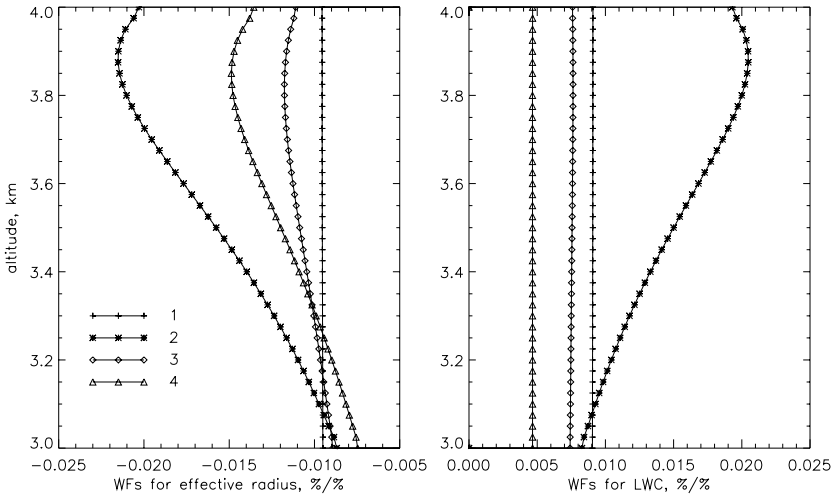

Fig. 6.12. Normalized layer-integrated WFs (layer geometrical thickness 50 m) for the relative variation of the effective radius of water droplets (left panel) and liquid water content (right panel) corresponding to the pair (LWC,r). Calculations were performed for the reflected solar radiance observed at TOA in nadir viewing geometry at a solar zenith angle of 45° at the following wavelengths: 1, 758.2 nm; 2, 760.425 nm; 3, 1.6 µm; 4, 2.2 µm. A vertically homogeneous water cloud with an optical thickness of 10 was assumed. The surface albedo was set to 0.3.

instead of the liquid water content. The corresponding WFs for the pair (N, r) are shown in Fig. 6.13. As clearly seen, WFs change the sign if (N, r) instead of (LWC,r) representation is used. This fact can be explained taking into account that LWC expressed via the particle number concentration and the effective radius of water droplets according to (6.154) is proportional to r^3. Therefore, in the spectral range where liquid water absorption is weak the scattering coefficient given by (6.139) is proportional to r^2. Thus, an increase of the effective radius of water droplets under assumption that the particle number concentration remains the same leads to an increase in the scattering coefficient and, therefore, in the cloud optical thickness which results, in turn, in an increase in the reflected radiation.

According to its definition, the weighting function provides a linear relationship between the variation of the corresponding parameter and the variation of the reflected or transmitted intensity. However, the intensity of the radiation depends nonlinearly on such cloud parameters as the particle number concentration and the effective radius of water droplets. The accuracy of the linear approximation depends on the magnitude of the parameter variation as well as on the observation geometry, on the solar zenith angle, on the cloud optical thickness, on the absorption of light within the cloud, etc. To investigate the accuracy of the linear approximation we assume that relative variations of all parameters are constant within the cloud. Under this assumption the relative

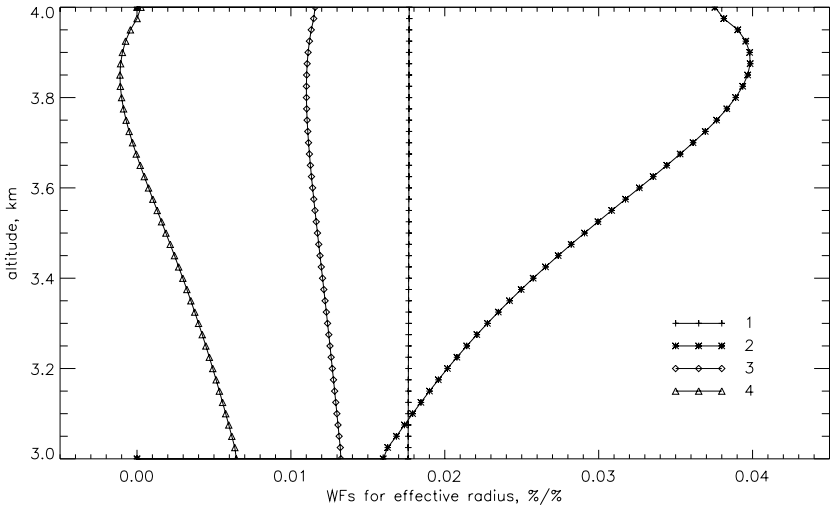

Fig. 6.13. Normalized layer-integrated WFs (layer geometrical thickness 50 m) for the relative variation of the effective radius of water droplets corresponding to the pair (N,r). Calculations were performed for the same conditions as in Fig. 6.12.

variation of the intensity can be expressed as follows:

$$\frac{\Delta I(\tau_v, \Omega_v)}{I(\tau_v, \Omega_v)} = \sum_{i=1}^{N_l} \mathcal{R}_p(\tau_i; \tau_v, \Omega_v) v_p \,, \tag{6.178}$$

where N_l is the number of layers within the cloud and subscript 'p' corresponds to the effective radius or to the particle number concentration. The relative variations of the reflected intensity corresponding to relative variations of the effective radius, v_r, and particle number concentration, v_N, in the range of 5–20% are shown in Fig. 6.14 and Fig. 6.15, respectively. The numerical values for intensity variations are calculated according to the following expression:

$$\frac{\Delta I(\tau_v, \Omega_v)}{I(\tau_v, \Omega_v; p)} = \frac{I(\tau_v, \Omega_v; p + \Delta p) - I(\tau_v, \Omega_v; p)}{I(\tau_v, \Omega_v; p)} \,, \tag{6.179}$$

where $I(\tau_v, \Omega_v; p)$ and $I(\tau_v, \Omega_v; p + \Delta p)$ are solutions of the radiative transfer equation corresponding to the parameters p and p + Δp, respectively.

The comparison of results presented in Figs 6.14 and 6.15 shows that the variations of the intensity calculated employing the linear approximation are systematically higher than the exact values. It follows as well that the linear approximation works better for variations of the particle number concentration. This is due to the fact that at least the water cloud scattering coefficient is the linear function of the particle number concentration whereas its dependence on the effective radius of water droplets is quadratic. The effect of the nonlinearity is especially pronounced in the spectral range where the liquid water absorption is strong. For example, as can be seen from Fig. 6.14, at 2.2 µm 20% variation

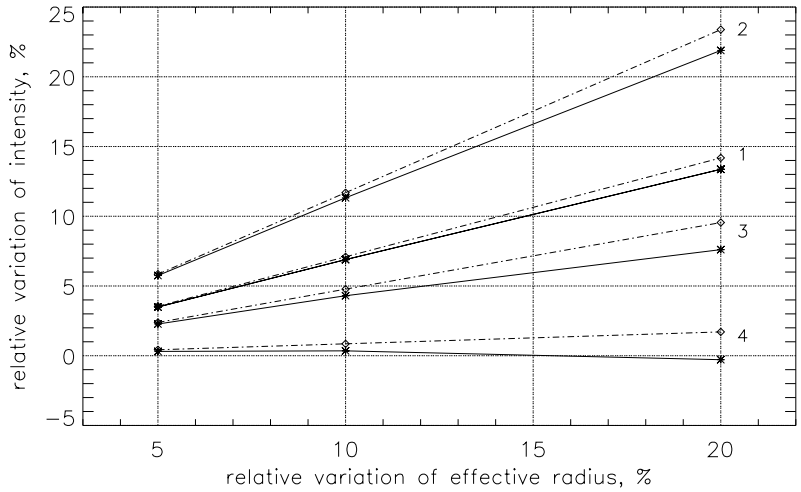

Fig. 6.14. Comparison of the relative variations of the reflected intensity caused by variations of the effective radius of water droplets. Solid line represents the results of numerical calculations and dash-dotted line corresponds to the linear approximation. The calculations were performed for a solar zenith angle of 45° and a surface albedo of 0.3 at the following wavelengths: 1, 758.2 nm; 2, 760.425 nm; 3, 1.6 μm; 4, 2.2 μm.

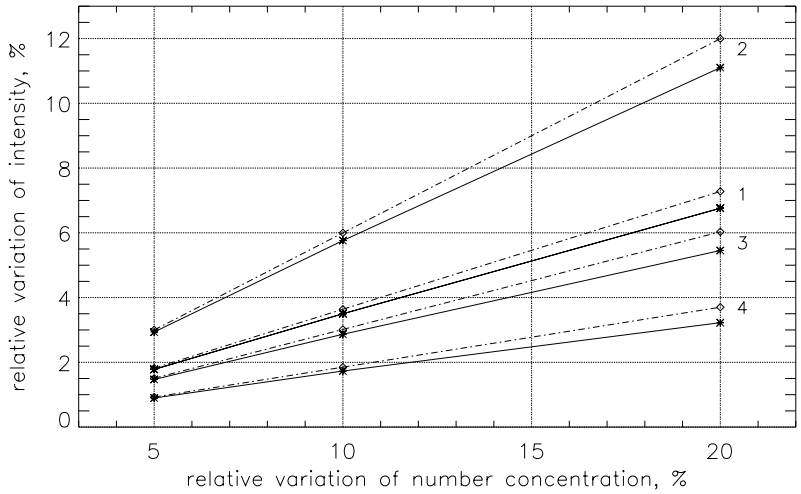

Fig. 6.15. Comparison of the relative variations of the reflected intensity caused by variations of the particle number concentration of water droplets. Solid line represents the results of numerical calculations and dash-dotted line corresponds to the linear approximation. The calculations were performed for a solar zenith angle of 45° and a surface albedo of 0.3 at the following wavelengths: 1, 758.2 nm; 2, 760.425 nm; 3, 1.6 μm; 4, 2.2 μm.

of the effective radius of water droplets results in the linear approximation in a variation of the intensity of about 1.8% whereas the exact value is even negative.

6.11 Application to the retrieval of the effective radius of water droplets

The weighting functions $\mathcal{W}_N(z; z_v, \Omega_v)$ and $\mathcal{W}_r^N(z; z_v, \Omega_v)$ can be used for the retrieval of the vertical profiles of $N(z)$ and $r(z)$ within a cloud. However, these functions considered as functions of the wavelength are highly correlated and a simultaneous retrieval of both parameters, i.e., $N(z)$ and $r_1(z)$ is a very complicated matter. Therefore, it is reasonable to assume that the optical thickness of the cloud, τ_c, can be estimated using the measured reflected radiation in the spectral range, where the gaseous and liquid water absorption is weak [7]. Let us use the retrieved optical thickness to estimate the particle number concentration. Obviously, we can not retrieve the profile of $N(z)$ since in the spectral ranges with weak gaseous and liquid water absorption the WF for the particle number concentration is almost independent of the altitude within the cloud (see Fig. 6.12). Therefore, we will assume that the shape of the particle number concentration is known *a priori* and only the scaling factor needs to be estimated. Namely, the unknown profile of the particle number concentration, $N'(z)$, will be approximated as follows:

$$N'(z) = CN(z)\,, \tag{6.180}$$

where $N(z)$ is the known shape of the particle number concentration and C is the scaling factor. Using (6.143) for the optical thickness of the cloud, we obtain the estimation for the scaling factor C as follows:

$$\hat{C} = \frac{\tau_c}{\int\limits_{z_b}^{z_t} e_1'(z)\,\mathrm{d}z}\,, \tag{6.181}$$

where τ_c is the estimated value of the cloud optical thickness. The extinction coefficient of water droplets, $e_1'(z)$, corresponds to the known shape of the particle number concentration $N(z)$ and an unknown profile of the effective radius $r_1'(z)$, which should be estimated as well. To obtain $\hat{C}$ according to (6.181), we take into account that in the linear approximation the extinction coefficient, $e_1'(z)$, corresponding to an unknown effective radius $r_1'(z)$ can be represented as follows:

$$e_1'(z) = e_1(z) + \frac{\partial e_1(z)}{\partial r_1(z)}\delta r_1(z)\,, \tag{6.182}$$

where the extinction coefficient, $e_1(z)$, corresponds to the known profile of the effective radius, $r_1(z)$, and $\delta r_1(z) = r_1'(z) - r_1(z)$. Substituting $e_1'(z)$ as given by (6.182) into (6.181), we obtain

$$\hat{C} = \frac{\tau_c}{\int\limits_{z_b}^{z_t} \Big[e_1(z) + \Delta e_1(z) \Big] \, \mathrm{d}z} \,. \tag{6.183}$$

Here, the variation of the extinction coefficient, $\Delta e_1(z)$, is caused by the variation of the effective radius, $\delta r_1(z)$, i.e.,

$$\Delta e_1(z) = \frac{\partial e_1(z)}{\partial r_1(z)} \delta r_1(z) \,. \tag{6.184}$$

Assuming that $\Delta e_1(z)$ is small compared to $e_1(z)$, it follows in the linear approximation:

$$\hat{C} = \frac{\tau_c}{\int\limits_{z_b}^{z_t} e_1(z) \, \mathrm{d}z} - \frac{\tau_c}{\Big[\int_{z_b}^{z_t} e_1(z) \, \mathrm{d}z \Big]^2} \int_{z_b}^{z_t} \Delta e_1(z) \, \mathrm{d}z \,. \tag{6.185}$$

The first term in this equation corresponds to the estimation of the scaling factor obtained ignoring the variation of the effective radius. Introducing the following definition for this scaling factor:

$$C[r_1(z)] = \frac{\tau_c}{\int\limits_{z_b}^{z_t} e_1(z) \, \mathrm{d}z} \,, \tag{6.186}$$

and substituting it into (6.185), we obtain

$$\hat{C} = C[r_1(z)] - \frac{C[r_1(z)]}{\int_{z_b}^{z_t} e_1(z) \, \mathrm{d}z} \int_{z_b}^{z_t} \frac{\partial e_1(z)}{\partial r_1(z)} \delta r_1(z) \, \mathrm{d}z \,. \tag{6.187}$$

Introducing for the simplification the function $E_1(z)$ as

$$E_1(z) = -\frac{1}{\int_{z_b}^{z_t} e_1(z) \, \mathrm{d}z} \frac{\partial e_1(z)}{\partial r_1(z)} r_1(z) \,, \tag{6.188}$$

Eq. (6.187) can be rewritten in the following form:

$$\hat{C} = C[r_1(z)] + C[r_1(z)] \int_{z_b}^{z_t} E_1(z) v_r(z) \, \mathrm{d}z \,, \tag{6.189}$$

where $v_r(z)$ is the relative variation of the effective radius of water droplets. Substituting now $\hat{C}$ given by (6.189) into (6.180) instead of C and introducing the zero-order estimation of the particle number concentration obtained ignoring the variation of the effective radius as

$$\bar{N}(z) = C[r_1(z)] N(z) \,, \tag{6.190}$$

we obtain an estimation for the particle number concentration accounting for the variation of the effective radius as follows:

$$N'(z) = \bar{N}(z) + \bar{N}(z) \int_{z_b}^{z_t} E_1(z) v_r(z)\, \mathrm{d}z\,. \tag{6.191}$$

This equation provides the following relationship between the relative variation of the particle number concentration around $\bar{N}(z)$ and the relative variation of the effective radius of water droplets:

$$v_N(z) = \frac{N'(z) - \bar{N}(z)}{\bar{N}(z)} = \int_{z_b}^{z_t} E_1(z) v_r(z)\, \mathrm{d}z\,. \tag{6.192}$$

The variation of the measured functional, $\delta\Phi(z_v, \Omega_v)$, in the spectral range containing absorption structures of the liquid water can be written now as follows:

$$\begin{aligned} \delta\Phi(z_v, \Omega_v) &= \Phi'(z_v, \Omega_v) - \Phi(z_v, \Omega_v) \\ &= \int_{z_b}^{z_t} \left[\mathcal{W}_N(z; z_v, \Omega_v) v_N(z) + \mathcal{W}_r^N(z; z_v, \Omega_v) v_r(z) \right] \sigma_e(z)\, \mathrm{d}z\,, \end{aligned} \tag{6.193}$$

where $\Phi'(z_v, \Omega_v)$ is the measured value and $\Phi(z_v, \Omega_v)$ is calculated for the particle number concentration $\bar{N}(z)$ and the effective radius $r_1(z)$. Substituting further $v_N(z)$ given by (6.192) into (6.193), we obtain the expression for the variation of the measured functional, $\delta\Phi(z_v, \Omega_v)$, containing only the effective radius of water droplets as unknown parameter:

$$\begin{aligned} \delta\Phi(z_v, \Omega_v) &= \int_{z_b}^{z_t} \left[\mathcal{W}_N(z; z_v, \Omega_v) \int_{z_b}^{z_t} E_1(z') v_r(z') dz' \right] \sigma_e(z)\, \mathrm{d}z \\ &+ \int_{z_b}^{z_t} \mathcal{W}_r^N(z; z_v, \Omega_v) v_r(z) \sigma_e(z)\, \mathrm{d}z\,. \end{aligned} \tag{6.194}$$

Introducing the specific weighting function for the effective radius in the following form:

$$\begin{aligned} \mathcal{W}_r^{\tau_c}(z; z_v, \Omega_v) &= \mathcal{W}_r^N(z; z_v, \Omega_v) \sigma_e(z) \\ &+ E_1(z) \int_{z_b}^{z_t} \mathcal{W}_N(z; z_v, \Omega_v) \sigma_e(z)\, \mathrm{d}z\,, \end{aligned} \tag{6.195}$$

we obtain

$$\delta\Phi(z_v, \Omega_v) = \int_{z_b}^{z_t} \mathcal{W}_r^{\tau_c}(z; z_v, \Omega_v) v_r(z)\, \mathrm{d}z\,. \tag{6.196}$$

This equation can be employed to estimate the vertical profile of the effective radius of water droplets using the measured radiation in the spectral range containing liquid water absorption bands, e.g., around 1.6, 2.2 or 3.7 µm.

6.12 Weighting functions for cloud geometrical parameters

In this section we derive the analytical expressions for geometrical cloud parameters such as the cloud top and cloud bottom height defining the position of a cloud layer in the atmosphere.

6.12.1 Theory

Let us assume that the variation of the measured functional, $\delta\Phi$, is caused by the variation of the cloud scattering, $s_k(\tau)$, and absorption, $a_k(\tau)$, coefficients only. Then according to (6.68) we have

$$\delta\Phi(\tau_v,\Omega_v)=\sum_{k=1}^{2}\int_0^{\tau_0}\Big[\mathcal{W}_{s_k}(\tau;\tau_v,\Omega_v)v_{s_k}(\tau)+\mathcal{W}_{a_k}(\tau;\tau_v,\Omega_v)v_{a_k}(\tau)\Big]\,\mathrm{d}\tau\,, \quad (6.197)$$

where $v_{s_k}(\tau)=\delta s_k(\tau)/s_k(\tau)$ and $v_{a_k}(\tau)=\delta a_k(\tau)/a_k(\tau)$ are the relative variations of the cloud scattering and absorption coefficients, respectively, and subscript $k=1$ corresponds to water droplets and $k=2$ to ice crystals. The expressions for WFs $\mathcal{W}_{a_k}(\tau;\tau_v,\Omega_v)$ and $\mathcal{W}_{s_k}(\tau;\tau_v,\Omega_v)$ are given by (6.92) and (6.97), respectively. To introduce the cloud geometrical parameters we rewrite at first (6.197) in the form containing the absolute variation of the cloud absorption and scattering coefficients as well as the integration over the altitude z instead of the optical depth τ:

$$\begin{aligned}\delta\Phi(z_v,\Omega_v) &= \sum_{k=1}^{2}\int_0^{H}\Bigg[\mathcal{W}_{s_k}(z;\tau_v,\Omega_v)\frac{\delta s_k(z)}{s_k(z)}\\ &+ \mathcal{W}_{a_k}(z;\tau_v,\Omega_v)\frac{\delta a_k(z)}{a_k(z)}\Bigg]\sigma_e(z)\,\mathrm{d}z\,, \quad (6.198)\end{aligned}$$

where H is the top of atmosphere altitude. Taking into account that the optical parameters of the cloud are non-zero within the cloud layer only, we can represent them in the following form:

$$p_k(z)=\Theta(z_t-z)\Theta(z-z_b)p_k(z)\,, \quad (6.199)$$

which allows us to define the cloud parameters in the entire atmosphere. Here, z_t and z_b are altitudes of the cloud top and bottom, respectively, function $p_k(z)$ is assumed to be the scattering or the absorption coefficient of the cloud, and functions $\Theta(z_t-z)$ and $\Theta(z-z_b)$ are the Heaviside step-functions given by (6.18).

Employing (6.199), variations of the cloud optical parameters caused by variations of the cloud top and bottom heights can be expressed in the linear approximation as follows:

$$\begin{aligned}\delta p_k(z) &= \left[\frac{\mathrm{d}\Theta(z_t-z)}{\mathrm{d}z_t}p_k(z)+\Theta(z_t-z)\frac{\mathrm{d}p_k(z)}{\mathrm{d}z_t}\right]\Theta(z-z_b)\Delta z_t\\ &+ \left[\frac{\mathrm{d}\Theta(z-z_b)}{\mathrm{d}z_b}p_k(z)+\Theta(z-z_b)\frac{\mathrm{d}p_k(z)}{\mathrm{d}z_b}\right]\Theta(z_t-z)\Delta z_b\,. \quad (6.200)\end{aligned}$$

Here, $dp_k(z)/dz_t$ and $dp_k(z)/dz_b$ are derivatives of the cloud parameters with respect to the cloud top and bottom height, respectively, $\Delta z_t=z_t'-z_t$ and $\Delta z_b=z_b'-z_b$ are the variations of CTH and CBH. Derivatives of the Heaviside

step-functions with respect to the cloud top height, z_t, and the cloud bottom height, z_b, can be obtained analytically [9]:

$$\frac{\mathrm{d}\Theta(z_t - z)}{\mathrm{d}z_t} = \delta(z_t - z)\,, \tag{6.201}$$

$$\frac{\mathrm{d}\Theta(z - z_b)}{\mathrm{d}z_b} = -\delta(z_b - z)\,, \tag{6.202}$$

where $\delta(z_t - z)$ and $\delta(z_b - z)$ are the Dirac δ-functions. Substituting these expressions into (6.200), dividing both sides of this equation by $p_k(z)$ and introducing for the simplification the following functions:

$$t_{p_k}(z) = \left[\delta(z_t - z) + \Theta(z_t - z)\frac{1}{p_k(z)}\frac{\mathrm{d}p_k(z)}{\mathrm{d}z_t}\right]\Theta(z - z_b)\,, \tag{6.203}$$

$$b_{p_k}(z) = \left[-\delta(z_b - z) + \Theta(z - z_b)\frac{1}{p_k(z)}\frac{\mathrm{d}p_k(z)}{\mathrm{d}z_b}\right]\Theta(z_t - z)\,, \tag{6.204}$$

we obtain

$$\frac{\delta p_k(z)}{p_k(z)} = t_{p_k}(z)\Delta z_t + b_{p_k}(z)\Delta z_b\,. \tag{6.205}$$

Substituting further these expressions into (6.198), we obtain the variation of the measured functional as a linear function with respect to the variations of CTH and CBH:

$$\delta\Phi(z_v, \Omega_v) \;=\; \int_0^H \Big[\mathcal{W}_{z_t}(z; \tau_v, \Omega_v)\Delta z_t + \mathcal{W}_{z_b}(z; \tau_v, \Omega_v)\Delta z_b\Big]\sigma_e(z)\,\mathrm{d}z\,, \tag{6.206}$$

where functions $\mathcal{W}_{z_t}(z; \tau_v, \Omega_v)$ and $\mathcal{W}_{z_b}(z; \tau_v, \Omega_v)$ are defined as follows:

$$\mathcal{W}_{z_t}(z; \tau_v, \Omega_v) = \sum_{k=1}^{2}\Big[t_{s_k}(z)\mathcal{W}_{s_k}(z; \tau_v, \Omega_v) + t_{a_k}(z)\mathcal{W}_{a_k}(z; \tau_v, \Omega_v)\Big]\,, \tag{6.207}$$

$$\mathcal{W}_{z_b}(z; \tau_v, \Omega_v) = \sum_{k=1}^{2}\Big[b_{s_k}(z)\mathcal{W}_{s_k}(z; \tau_v, \Omega_v) + b_{a_k}(z)\mathcal{W}_{a_k}(z; \tau_v, \Omega_v)\Big]\,, \tag{6.208}$$

and functions $t_{s_k}(z)$, $t_{a_k}(z)$ and $b_{s_k}(z)$, $b_{a_k}(z)$ are given by (6.203) and (6.204) for $p_k(z) = s_k(z)$ and $p_k(z) = a_k(z)$, respectively. Thus, we obtain the following expressions for CTH and CBH weighting functions:

$$\mathcal{W}_{z_t}(z_v, \Omega_v) = \int_0^H \mathcal{W}_{z_t}(z; \tau_v, \Omega_v)\sigma_e(z)\,\mathrm{d}z\,, \tag{6.209}$$

$$\mathcal{W}_{z_b}(z_v, \Omega_v) = \int_0^H \mathcal{W}_{z_b}(z; \tau_v, \Omega_v)\sigma_e(z)\,\mathrm{d}z\,. \tag{6.210}$$

The derived expressions can be used to calculate the weighting functions after the expressions for functions $t_{p_k}(z)$ and $b_{p_k}(z)$ containing derivatives of the cloud

optical parameters with respect to CTH and CBH having been obtained. For this reason we will first derive a general expression for derivatives of the cloud optical parameters with respect to CTH assuming that the actual value of a certain parameter is obtained scaling the known shape profile:

$$p_k(z) = c_k p_h(z)\,, \tag{6.211}$$

where $p_h(z)$ is the shape profile of the corresponding parameter and c_k is a scaling factor. The scaling factor is obtained to match the corresponding integral parameter such as the optical thickness or liquid water path of a cloud.

The derivative $\partial p_k(z)/\partial z_t$ can be obtained using (6.211) as follows:

$$\frac{\partial p_k(z)}{\partial z_t} = \frac{\partial}{\partial z_t}\Big[c_k p_h(z)\Big] = \left[\frac{\partial c_k}{\partial z_t} p_h(z) + c_k \frac{\partial p_h(z)}{\partial z_t}\right]. \tag{6.212}$$

Assuming that the scaling factor is chosen to match the optical thickness of the cloud, the derivative $\partial c_k/\partial z_t$ can be found as

$$\frac{\partial c_k}{\partial z_t} = \frac{\partial}{\partial z_t}\Big[\frac{\tau_c}{\tau_{p_h}}\Big] = -\frac{\tau_c}{\tau_{p_h}^2}\frac{\partial \tau_{p_h}}{\partial z_t}\,, \tag{6.213}$$

where we have taken into account that τ_c is a given constant value of the cloud optical thickness. To find the analytical expression for the derivative $\partial\tau_{p_h}/\partial z_t$ we use the following relationship:

$$\int_0^1 p_h(x)\,\mathrm{d}x \equiv \frac{1}{L}\int_{z_b}^{z_t} p_h(z)\,\mathrm{d}z = \frac{\tau_{p_h}}{L}\,, \tag{6.214}$$

where x is the dimensionless altitude given by (6.126), and $L = z_t - z_b$ is the geometrical thickness of the cloud. Differentiating (6.214) with respect to the parameter z_t, we obtain

$$-\frac{1}{L^2}\tau_{p_h} + \frac{1}{L}\frac{\partial \tau_{p_h}}{\partial z_t} = 0 \quad\Longrightarrow\quad \frac{\partial \tau_{p_h}}{\partial z_t} = \frac{\tau_{p_h}}{L}\,. \tag{6.215}$$

Substituting the obtained result into (6.213), we have

$$\frac{\partial c_k}{\partial z_t} = -\frac{\tau_c}{\tau_{p_h} L}\,. \tag{6.216}$$

For the derivative $\partial p_h(z)/\partial z_t$ we obtain

$$\frac{\partial p_h(z)}{\partial z_t} = \frac{\partial p_h(z)}{dz}\,\frac{\partial z}{\partial x}\,\frac{\partial x}{\partial z_t} = -\frac{\partial p_h(z)}{\partial z}(1-x)\,. \tag{6.217}$$

Taking into account that the dimensionless altitude x is given by (6.126) and substituting it into the previous equation, we obtain

$$\frac{\partial p_h(z)}{\partial z_t} = -\frac{\partial p_h(z)}{\partial z}\frac{z - z_b}{L}\,. \tag{6.218}$$

Substituting (6.216) and (6.218) into (6.212), it follows that

$$\frac{\partial p_k(z)}{\partial z_t} = \left[-\frac{\tau_c}{\tau_{p_h} L} p_h(z) - c_k \frac{\partial p_h(z)}{\partial z} \frac{z - z_b}{L} \right] . \tag{6.219}$$

Taking into account (6.211), we obtain the final expression for the derivative of the optical parameters with respect to CTH as follows:

$$\frac{\partial p_k(z)}{\partial z_t} = -\frac{1}{L} \left[p_k(z) + \frac{\partial p_k(z)}{\partial z} (z - z_b) \right] . \tag{6.220}$$

Employing the same approach, the derivative of the optical parameters with respect to CBH is obtained in the following form:

$$\frac{\partial p_k(z)}{\partial z_b} = \frac{1}{L} \left[p_k(z) - \frac{\partial p_k(z)}{\partial z} (z_t - z) \right] . \tag{6.221}$$

The first term in the derived expressions results from the dependence of the scaling factor on the cloud geometrical parameters and the second contains the derivative of the corresponding parameter with respect to the altitude. Substituting (6.220) and (6.221) into (6.203) and (6.204), we obtain the final expressions for functions $t_{p_k}(z)$ and $b_{p_k}(z)$ in the following form:

$$\begin{aligned} t_{p_k}(z) &= \left\{ \delta(z_t - z) - \frac{\Theta(z_t - z)}{L} \left[1 + \frac{\partial \ln p_k(z)}{\partial z} (z - z_b) \right] \right\} \\ &\times \Theta(z - z_b) , \end{aligned} \tag{6.222}$$

$$\begin{aligned} b_{p_k}(z) &= \left\{ -\delta(z_b - z) + \frac{\Theta(z - z_b)}{L} \left[1 - \frac{\partial \ln p_k(z)}{\partial z} (z_t - z) \right] \right\} \\ &\times \Theta(z_t - z) . \end{aligned} \tag{6.223}$$

In some special cases the obtained expressions can be simplified. For example, for a vertically homogeneous cloud derivatives of the cloud scattering and absorption coefficients with respect to the altitude are zero. Thus, we obtain the following expressions for functions $t_{p_k}(z)$ and $b_{p_k}(z)$:

$$t_{p_k}(z) = \left[\delta(z_t - z) - \frac{\Theta(z_t - z)}{L} \right] \Theta(z - z_b) , \tag{6.224}$$

$$b_{p_k}(z) = \left[-\delta(z_b - z) + \frac{\Theta(z - z_b)}{L} \right] \Theta(z_t - z) . \tag{6.225}$$

Further simplification can be obtained if the optical parameters in an vertically homogeneous cloud are not rescaled for varying geometrical parameters. In this case we have

$$t_{p_k}(z) = \delta(z_t - z) \Theta(z - z_b) , \tag{6.226}$$

$$b_{p_k}(z) = -\delta(z_b - z) \Theta(z_t - z) , \tag{6.227}$$

and the weighting functions for CTH and CBH given by (6.209) and (6.210) can be rewritten as follows:

$$\mathcal{W}_{z_t}(z_v,\Omega_v)=\sum_{k=1}^{2}\Big[\mathcal{W}_{s_k}(z_t;\tau_v,\Omega_v)+\mathcal{W}_{a_k}(z_t;\tau_v,\Omega_v)\Big]\sigma_e(z_t)\,, \tag{6.228}$$

$$\mathcal{W}_{z_b}(z_v,\Omega_v)=-\sum_{k=1}^{2}\Big[\mathcal{W}_{s_k}(z_b;\tau_v,\Omega_v)+\mathcal{W}_{a_k}(z_b;\tau_v,\Omega_v)\Big]\sigma_e(z_b)\,. \tag{6.229}$$

Having defined the weighting functions for CTH and CBH, we can easily obtain WFs for other parameters characterizing the cloud geometry. In particular, the WF for the geometrical thickness of the cloud is

$$\mathcal{W}_{gt}(z_v,\Omega_v)=\mathcal{W}_{z_t}(z_v,\Omega_v)-\mathcal{W}_{z_b}(z_v,\Omega_v)\,. \tag{6.230}$$

Assuming that the cloud geometrical thickness is constant, we can obtain the WF characterizing the position of the cloud in the atmosphere as well. In this case the shift of a cloud can be described by simultaneous variations of the same magnitude of both CTH and CBH. Therefore, WF for the position of a cloud can be written as follows:

$$\mathcal{W}_{sh}(z_v,\Omega_v)=\mathcal{W}_{z_t}(z_v,\Omega_v)+\mathcal{W}_{z_b}(z_v,\Omega_v)\,. \tag{6.231}$$

6.12.2 Numerical results

In this subsection we consider examples of WFs for different cloud geometrical parameters corresponding to vertically homogeneous and inhomogeneous water clouds as well as to mixed clouds consisting of water droplets and ice crystals. At first we compare WFs for CTH and CBH obtained employing the analytical expressions derived in the previous subsection to results of the numerical calculations. For this purpose we consider the most general case of a vertically inhomogeneous mixed cloud consisting of water droplets and ice crystals. Corresponding vertical profiles of the liquid and ice water contents are shown in Fig. 6.16. The vertical profiles of the effective radius of water droplets and ice crystals were assumed to change linearly within the cloud. At the top of the cloud the effective radii of water droplets and ice crystals were set to 6 µm and 70 µm, respectively, and at the bottom of the cloud to 2 µm and 120 µm, respectively. The scattering and absorption coefficients of water droplets and ice crystals were calculated according to the analytical expressions given by (6.139)–(6.142). The numerical WFs were obtained using the numerical perturbation approach as follows:

$$\mathcal{W}_{z_t}(z_v,\Omega_v)=\frac{I(0,\Omega_v,z_t+\Delta z_t)-I(0,\Omega_v,z_t)}{\Delta z_t}\,, \tag{6.232}$$

where $I(0,\Omega_v,z_t)$ and $I(0,\Omega_v,z_t+\Delta z_t)$ are the reflected intensities at the top of the atmosphere corresponding to the cloud top height z_t and $z_t+\Delta z_t$, respectively, and Δz_t is the perturbation of the cloud top height which was set to 0.01 km.

The simulated spectrum of the reflected solar radiation observed at TOA in the nadir viewing geometry in the presence of a homogeneous water cloud

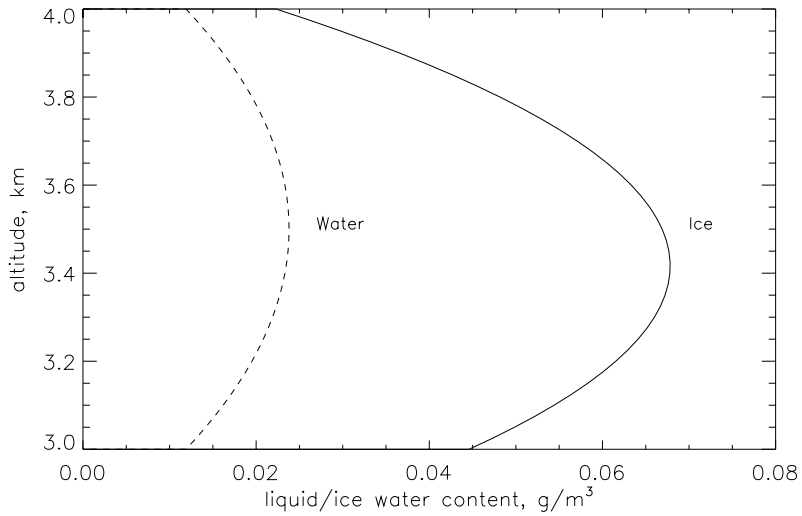

Fig. 6.16. Vertical profiles of the liquid and ice water contents for a mixed cloud having an optical thickness of 10.

having an optical thickness of 10 is shown in Fig. 6.17. The calculations were performed for a finite spectral resolution assuming the instrument slit function to be the boxcar function with a full width of 0.1 nm. Relative differences between the reflected intensities corresponding to a homogeneous and an inhomogeneous water cloud as well as to a homogeneous and a mixed cloud are shown in the lower panel of Fig. 6.17. As can clearly be seen, at spectral points where the gaseous absorption is week the difference between reflected intensities corresponding to a vertically homogeneous and a vertically inhomogeneous water cloud is very small whereas, due to a difference in the phase functions, the reflected intensity in a presence of a mixed cloud is approximately 2% higher than for a homogeneous water cloud of the same optical thickness.

Similarly to the parameters discussed in previous sections let us introduce the normalized WFs for CTH and CBH which are numerically equivalent to relative variations of the observed intensity caused by 1 km variations of CTH or CBH, respectively. For example, the normalized weighting function for CTH is introduced as

$$\frac{\Delta I(\tau_v, \Omega_v)}{I(\tau_v, \Omega_v)} = \frac{\mathcal{W}_{z_t}(z_v, \Omega_v)}{I(\tau_v, \Omega_v)} \Delta z_t = \mathcal{R}_{z_t}(z_v, \Omega_v) \Delta z_t \,. \tag{6.233}$$

The normalized weighting functions for CTH and CBH in the spectral range of the O_2-A absorption band obtained employing analytical expressions, Eqs (6.209) and (6.210), as well as calculated using the numerical perturbation approach as given by (6.232) are shown in Fig. 6.18. Good agreement between the numerical and analytical weighting functions confirms the correctness of the derived general analytical expressions. Although the overall wavelength behavior of both weighting functions is similar, it is clearly seen that the fine spectral structure is

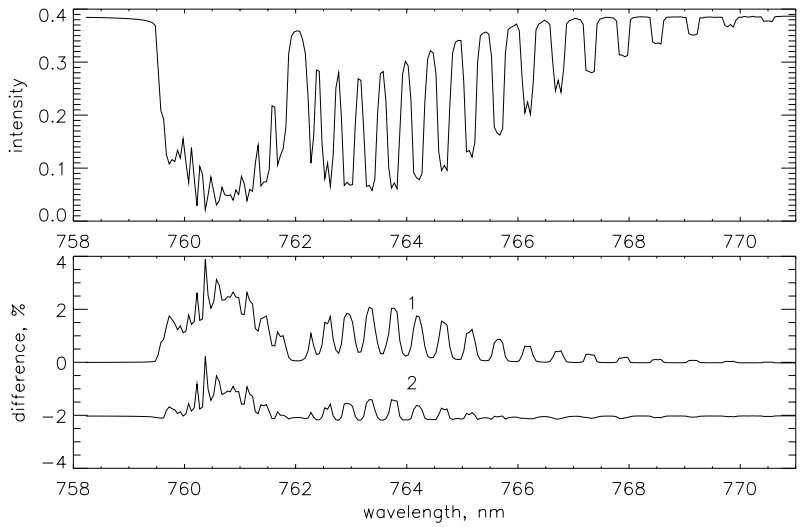

Fig. 6.17. Upper panel: reflected intensity at TOA for a homogeneous water cloud. Lower panel: relative differences between the reflected intensities for: 1, homogeneous and inhomogeneous water cloud, 2, homogeneous and mixed cloud ($\tau_{\text{water}} = 9$, $\tau_{\text{ice}} = 1$). Calculations were performed for a solar zenith angle of 45° and a surface albedo of 0.3.

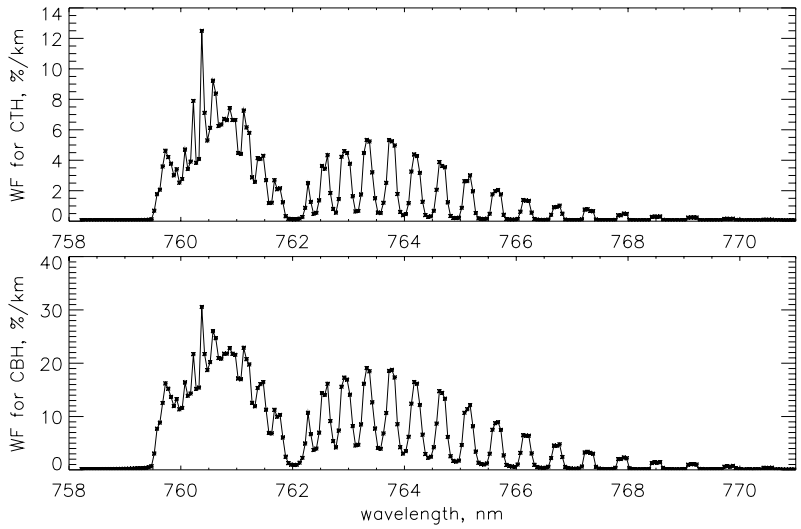

Fig. 6.18. Comparison of the numerical (symbols) and the normalized layer integrated analytical (solid line) WFs for the cloud top (upper panel) and cloud bottom height (lower panel) in a presence of a mixed cloud of optical thickness 10. The calculations were performed for a solar zenith angle of 45° and a surface albedo of 0.3.

significantly different, i.e, the spectral structures of the reflected intensity variations caused by variations of CTH and CBH are different and, thus, these parameters can be considered to be independent. As seen from the plot, CTH and CBH weighting functions are very small in spectral intervals where O_2 absorption is weak which is in accordance with the well known fact that in a non-absorbing atmosphere the reflection of the cloud is independent of its altitude and geometrical thickness. Since both weighting functions are always positive, an increase of CTH or CBH under the assumption of constant optical thickness leads to an enhancement in the reflected intensity. In particular, as follows from Fig. 6.18, the relative variation of the reflected intensity due to a 1 km shift of CTH or CBH reaches about 13% and 30%, respectively. The reflected intensity is most sensitive to variations of CTH and CBH in spectral ranges where the gaseous absorption is strong.

In the most general case of a vertically inhomogeneous mixed cloud the weighting functions for CTH and CBH contain derivatives of vertical profiles of the scattering and absorption coefficients with respect to the altitude (see Eqs (6.222) and (6.223) for the auxiliary functions $t_{p_k}(z)$ and $b_{p_k}(z)$, respectively). Therefore, WFs depend on the vertical structure of the cloud, i.e., on the vertical distribution of the scattering and absorption coefficients within the cloud. Nevertheless, due to a lack of information on the cloud structure, retrievals of the cloud top height from real measurements are often performed assuming the cloud to be vertically homogeneous. The validity of this approximation can be investigated analyzing the influence of the cloud vertical inhomogeneity on the weighting functions. This was done comparing CTH WF for a vertically homogeneous water cloud to that for vertically inhomogeneous water and mixed clouds. If the geometrical thickness of the cloud is known, the inverse problem can be simplified because the variation of the reflected intensity is resulted only from a variation of the vertical position of the cloud, i.e., of the cloud altitude, and the corresponding WF is given by (6.231). The cloud altitude weighting functions describing the simplified inverse problem were also compared in the similar manner as CTH WFs. The comparison was performed for the cloud optical thickness of 10. For mixed clouds the optical thicknesses of water droplets and ice crystals were selected to be 9 and 1, respectively.

Figure 6.19 illustrates the sensitivity of the weighting functions for the cloud top height (curves 1 and 2) and the cloud altitude (curves 3 and 4) to the vertical inhomogeneity of a cloud. The ratios of WFs for a vertically homogeneous water cloud to WFs for an inhomogeneous water cloud are shown by dashed lines and the ratios of WFs for a vertically homogeneous water cloud to WFs for an inhomogeneous mixed cloud are represented by solid lines. As can clearly be seen, in the considered observation geometry CTH WF for a vertically homogeneous cloud is much larger than that for both inhomogeneous water clouds and mixed clouds, whereas in the case of a constant geometrical thickness the influence of the vertical cloud inhomogeneity is substantially weaker. Therefore, an estimation of the cloud top height under the assumption of the vertical homogeneity of a cloud is more accurate in the case of a known geometrical thickness of the cloud.

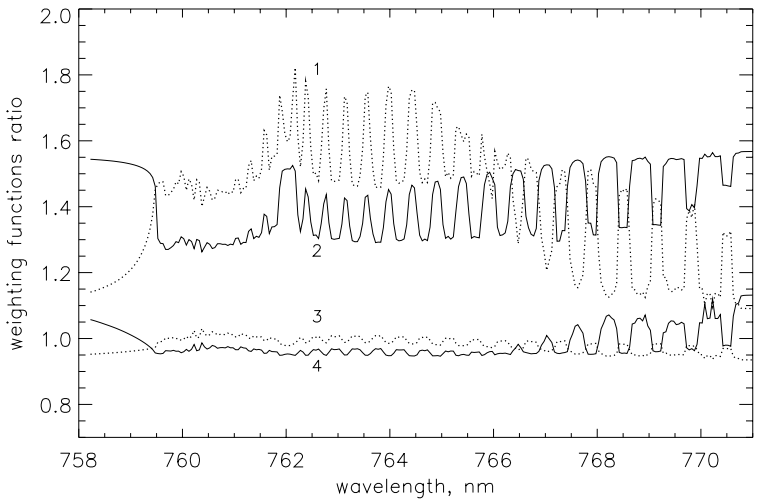

Fig. 6.19. Comparison of the weighting functions for the cloud top height (curves 1 and 2) and the cloud altitude (curves 3 and 4). Dashed lines: ratios of WFs for a vertically homogeneous water cloud to WFs for a inhomogeneous water cloud. Solid lines: ratios of WFs for a vertically homogeneous water cloud to WFs for a inhomogeneous mixed cloud.

A variation of the reflected intensity in a cloudy atmosphere can be caused not only by variations of the cloud altitude, cloud top or bottom height, or vertical distributions of cloud parameters, but also by variations of the pressure and temperature. In spectral regions where the gaseous absorption is not negligible, variations of the pressure and temperature in the atmosphere cause variations of the absorption cross-sections of atmospheric gases and, thus, alter the absorption of the solar radiation. Fig. 6.20 illustrates contributions into the relative variation of the observed intensity due to 1% variation of the pressure, 1 K variation of the temperature, and 100 m variation of the cloud top height. As clearly seen, all plotted variations are of the same magnitude providing an estimation for the error propagation in the case of uncertain atmospheric parameters.

Concluding the discussion of WFs for cloud geometrical parameters let us consider the cloud top height weighting functions for a two-layered cloud system. The cloud system was assumed to comprise an ice crystal cloud with a cloud top height of 8 km in the upper layer and a water cloud with a cloud top height of 4 km in the lower layer. Both cloud layers were assumed to have a geometrical thickness of 1 km. Corresponding WFs in the O_2-A absorption band are shown in Fig. 6.21 for different optical thicknesses of cloud layers. As can be seen from the plot, the spectral structure and magnitude of CTH WFs for the upper and lower cloud layers are strongly dependent on the distribution of the optical thickness between the cloud layers. For example, if the optical thickness of the upper layer is much smaller than that of the lower layer, 1 km variation of the cloud top height of the lower layer results in a relative variation of the reflected intensity of

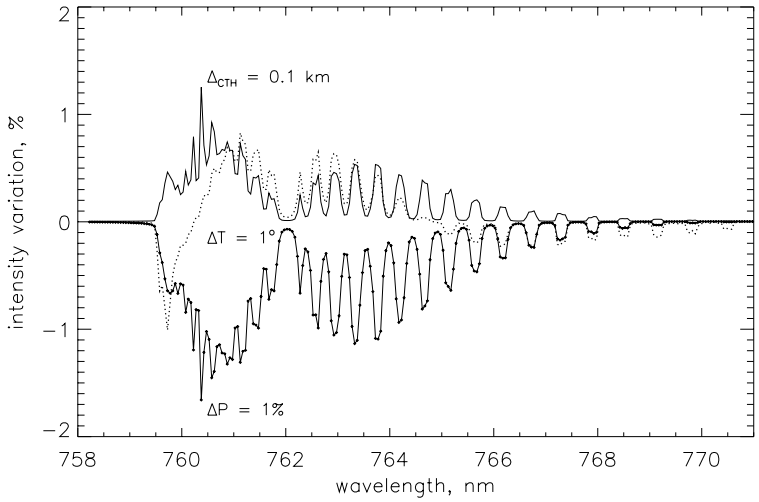

Fig. 6.20. Relative variations of the reflected intensity in a presence of a mixed cloud due to 1% variation of the pressure, 1 K variation of the temperature, and 100 m variation of the cloud top height.

about 11% at wavelengths around 760.4 nm (upper panel in Fig. 6.21), whereas, the relative variation of the reflected intensity caused by the same variation of CTH of the upper layer is about a factor of 5 smaller. An increase in the optical thickness of the upper cloud layer for a constant total optical thickness leads to an increase in CTH WF of the upper cloud layer and a decrease in CTH WF of the lower cloud layer (lower panel in Fig. 6.21). Thus, in the case of a two-layered cloud system the reflected solar radiance observed within a gaseous absorption band spectral range contains an information about the cloud top heights of both cloud layers. However, the retrieval of these parameters requires independent information about optical thicknesses of the upper and lower cloud layers.

6.13 Conclusion

Generally, to find a solution of an inverse problem, the weighting functions of the atmospheric parameters of interest are required. In this chapter we have extensively discussed the weighting functions not only for common atmospheric parameters, such as atmospheric trace gas number densities, pressure, temperature, and aerosol particle number density, but also for various cloud parameters, such as geometrical thickness, cloud top and bottom height, liquid water content and effective radius of water droplets and ice crystals. All obtained expressions for the weighting functions are implemented in the software package SCIATRAN 2.1 [26] and verified against the numerical perturbation technique. SCIATRAN 2.1 is freely available for non-commercial use at *www.iup.physik.uni-bremen.de/sciatran*. A brief description of the mathematical background of the

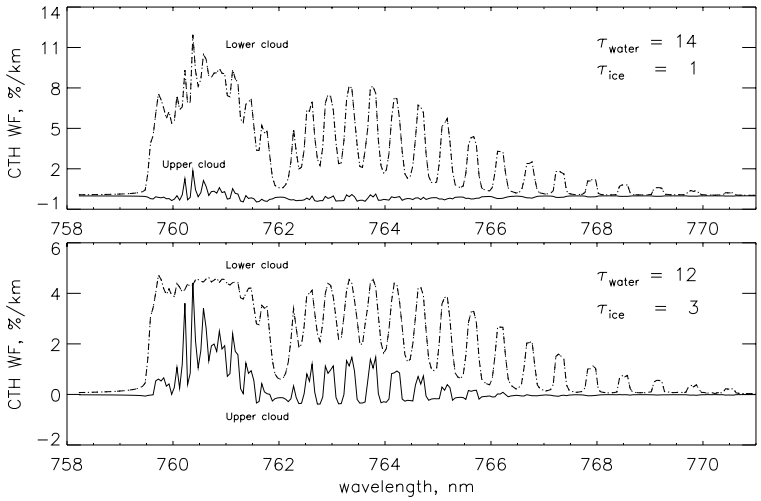

Fig. 6.21. Cloud top height weighting functions for a two-layered cloud system. The calculations were performed for the reflected intensity observed at TOA at a solar zenith angle of 45° and a surface albedo of 0.3. The cloud system was assumed to comprise an ice crystal cloud with a cloud top height of 8 km in the upper layer and a water cloud with a cloud top height of 4 km in the lower layer. Both cloud layers were assumed to have a geometrical thickness of 1 km. The total optical thickness of the cloud system was set to 15.

linearized radiative transfer equation, adjoint radiative transfer equation, and adjoint approach, as well as detailed derivation of the expressions for the weighting functions presented in this chapter, is aimed to facilitate the usage of the software package SCIATRAN 2.1 to solve various practical inverse problems.

The fact that, due to linearization errors, most of inverse problems need to be solved iteratively requiring an update of the forward intensity and weighting functions at each iterative step, was accounted for in the SCIATRAN 2.1 software package coupling the retrieval block with the radiative transfer model. The retrieval block, which was originally developed to retrieve vertical distributions or column amounts of atmospheric species, incorporates various inversion techniques such as the optimal estimation [19], Tikhonov regularization [28], and information operator approach [10], and can be adapted by a user to solve various inverse problems arising in remote sensing of the Earth's atmosphere. One of the retrieval block extensions already implemented in the inversion procedure is a retrieval of the cloud top height using satellite measurements of the backscattered solar radiation in the oxygen absorption A-band [21]. Some examples of successful applications of the SCIATRAN software package to the retrieval of vertical profiles of NO_2 and BrO as well as vertical columns of CH_4 and CO_2 using SCIAMACHY measurements are presented in [3, 23].

Acknowledgments

This work has been funded in parts by the German Ministry of Education and Research BMBF (grant 07UFE12/8) and the German Aerospace Center DLR (grant 50EE0027).

Appendix A: Derivation of weighting functions for main parameters

Extinction coefficient. For a variation of the extinction coefficient, we have: $p(\tau) = \sigma_e(\tau)$. Functions Y_e and G_e are given by Eqs (6.59) and (6.60). In the considered case they can be written as follows:

$$Y_e(\tau,\Omega) = \sigma_e(\tau)\left[\frac{\partial S_e(\tau,\Omega)}{\partial\sigma_e(\tau)} - \frac{\partial L_e}{\partial\sigma_e(\tau)}I\right] = -\sigma_e(\tau)\frac{\partial L_e}{\partial\sigma_e(\tau)}I\,, \quad (6.234)$$

$$G_e(\Omega) = \sigma_e(\tau)\left[\frac{\partial S_b(\Omega)}{\partial\sigma_e(\tau)} - \frac{\partial L_b}{\partial\sigma_e(\tau)}I\right] = 0\,, \quad (6.235)$$

where we have taken into account that functions S_e and S_b as well as the operator L_b as given by Eqs (6.15), (6.23) and (6.17), respectively, are independent of the extinction coefficient. We note that the extinction coefficient and the single scattering albedo are considered to be independent parameters. Substituting Eqs (6.234) and (6.235) into Eq. (6.61), we obtain

$$\Psi_e(\tau,\Omega) = -\sigma_e(\tau)\frac{\partial L_e}{\partial\sigma_e(\tau)}I\,. \quad (6.236)$$

The partial derivative of the operator L_e as given by Eq. (6.13) with respect to the extinction coefficient $\sigma_e(\tau)$ can be obtained as

$$\frac{\partial L_e}{\partial\sigma_e(\tau)} = \frac{\partial}{\partial\sigma_e(\tau)}\left[-\frac{\mu}{\sigma_e(z)}\frac{\mathrm{d}}{\mathrm{d}z}\right] = \frac{\mu}{\sigma_e^2(\tau)}\frac{\mathrm{d}}{\mathrm{d}z} = -\frac{\mu}{\sigma_e(\tau)}\frac{\mathrm{d}}{\mathrm{d}\tau}\,, \quad (6.237)$$

where we have used that $\mathrm{d}\tau = -\sigma_e(\tau)\,\mathrm{d}z$. Substituting Eq. (6.237) into Eq. (6.236), we obtain

$$\Psi_e(\tau,\Omega) = \mu\frac{\mathrm{d}I}{\mathrm{d}\tau}\,. \quad (6.238)$$

Substituting into this equation $\mu\,\mathrm{d}I/\mathrm{d}\tau$ as given by Eq. (6.9), the final expression for the auxiliary function $\Psi_e(\tau,\Omega)$ is written as follows:

$$\Psi_e(\tau,\Omega) = -I(\tau,\Omega) + J(\tau,\Omega) + S_e(\tau,\Omega)\,, \quad (6.239)$$

where $J(\tau,\Omega)$ and $S_e(\tau,\Omega)$ are given by Eqs (6.12) and (6.15), respectively. The final expression for the extinction coefficient WF follows after substitution the function $\Psi_e(\tau,\Omega)$ into Eq. (6.71):

$$\mathcal{W}_e(\tau;\tau_v,\Omega_v) = \int_{4\pi} I^*(\tau,\Omega;\Omega_v)\Big[J(\tau,\Omega) + S_e(\tau,\Omega) - I(\tau,\Omega)\Big]\,\mathrm{d}\Omega\,. \quad (6.240)$$

Single scattering albedo. Employing the same approach for a variation of the single scattering albedo, we obtain

$$\Psi_\omega(\tau,\Omega) = \omega(\tau)\left[\frac{\partial S_e(\tau,\Omega)}{\partial\omega(\tau)} - \frac{\partial L_e}{\partial\omega(\tau)}I\right], \tag{6.241}$$

where we have taken into account that the function S_b and the operator L_b as given by Eqs (6.23) and (6.17), respectively, are independent of the single scattering albedo and, therefore, $G_\omega(\Omega) = 0$. Taking into account Eqs (6.13) and (6.15), partial derivatives of the function S_e and of the operator L_e with respect to the single scattering albedo can be written as follows:

$$\frac{\partial S_e}{\partial\omega(\tau)} = -B(\tau)\,, \qquad \frac{\partial L_e}{\partial\omega(\tau)} = -\frac{1}{4\pi}\int_{4\pi} \mathrm{d}\Omega' p(\tau,\Omega,\Omega')\otimes\,. \tag{6.242}$$

Substituting these expressions into Eg. (6.241), we obtain the final expression for the auxiliary function $\Psi_\omega(\tau,\Omega)$:

$$\Psi_\omega(\tau,\Omega) = J(\tau,\Omega) - B(\tau)\omega(\tau)\,. \tag{6.243}$$

The final expression for the extinction coefficient WF follows after substitution the function $\Psi_\omega(\tau,\Omega)$ into Eq. (6.71):

$$\mathcal{W}_\omega(\tau;\tau_v,\Omega_v) = \int_{4\pi} I^*(\tau,\Omega;\Omega_v)\Big[J(\tau,\Omega) - B(\tau)\omega(\tau)\Big]\,\mathrm{d}\Omega\,, \tag{6.244}$$

Surface albedo. A variation of the surface albedo, A, causes only a variation of the lower boundary condition operator, L_b, as given by Eq. (6.17). Therefore, using Eqs (6.59)–(6.61), the expression for the function $\Psi_A(\tau,\Omega)$ can be written as follows:

$$\Psi_A(\tau,\Omega) = -A\psi_b(\tau,-\mu)\frac{\partial L_b}{\partial A}I\,. \tag{6.245}$$

Considering the operator L_b given by Eq. (6.17) as a function of the surface albedo, the partial derivative of the L_b with respect to A can be found in the following form:

$$\frac{\partial L_b}{\partial A} = -\frac{1}{\pi}\int_0^{\tau_0}\mathrm{d}\tau\delta(\tau-\tau_0)\int\limits_{4\pi}\mathrm{d}\Omega'\lambda(\mu')\rho(\Omega,\Omega')\otimes\,. \tag{6.246}$$

Applying this operator to the intensity $I(\tau,\Omega)$ and substituting the result into Eq. (6.245), we obtain

$$\Psi_A(\tau,\Omega) = \psi_b(\tau,-\mu)\frac{A}{\pi}\int\limits_{\Omega_+}\rho(\Omega,\Omega')I(\tau_0,\Omega')\mu'\,\mathrm{d}\Omega'\,. \tag{6.247}$$

Having defined the auxiliary function for the surface albedo, the corresponding WF can be obtained substituting it into Eq. (6.70):

$$\mathcal{W}_A(\tau_v,\Omega_v)=\frac{A}{\pi}\int_0^{\tau_0}\int_{4\pi} I^*(\tau,\Omega;\Omega_v)\psi_b(\tau,-\mu)F(\Omega,\tau_0)\,\mathrm{d}\Omega\,\mathrm{d}\tau\,, \qquad (6.248)$$

where the function

$$F(\Omega,\tau_0)=\int\limits_{\Omega_+}\rho(\Omega,\Omega')I(\tau_0,\Omega')\mu'\mathrm{d}\Omega' \qquad (6.249)$$

is introduced for the simplification reason. The final expression for the surface albedo WF follows after substitution the function $\psi_b(\tau,-\mu)$ given by Eq. (6.28) into Eq. (6.248). Taking into account properties of the Dirac δ-function and the Heaviside step-function, we obtain

$$\mathcal{W}_A(\tau_v,\Omega_v)=-\frac{A}{\pi}\int_{\Omega_-} I^*(\tau_0,\Omega;\Omega_v)F(\Omega,\tau_0)\mu\,\mathrm{d}\Omega\,, \qquad (6.250)$$

Surface emissivity. A variation of the surface emissivity, ϵ, causes only a variation of the function $S_b(\Omega)$ given by Eq. (6.23). Therefore, taking into account Eqs (6.59)–(6.61), the expression for the function $\Psi_\epsilon(\tau,\Omega)$ can be written as follows:

$$\Psi_\epsilon(\tau,\Omega)=\epsilon\psi_b(\tau,-\mu)\frac{\partial S_b(\Omega)}{\partial\epsilon}\,. \qquad (6.251)$$

The derivative of the function S_b with respect to the surface emissivity is

$$\frac{\partial S_b(\Omega)}{\partial\epsilon}=B(T_s)\,. \qquad (6.252)$$

Substituting Eq. (6.252) into Eq. (6.251), we obtain

$$\Psi_\epsilon(\tau,\Omega)=\psi_b(\tau,-\mu)\epsilon B(T_s)\,. \qquad (6.253)$$

Having defined the auxiliary function for the surface emissivity, the corresponding WF can be obtained substituting it into general expression for the scalar-parameter WF given by Eq. (6.70):

$$\mathcal{W}_\epsilon(\tau_v,\Omega_v)=\epsilon B(T_s)\int_0^{\tau_0}\int_{4\pi} I^*(\tau,\Omega;\Omega_v)\psi_b(\tau,-\mu)\,\mathrm{d}\Omega\,\mathrm{d}\tau\,. \qquad (6.254)$$

The final expression for the surface emissivity WF can be obtain in a way analogous to the surface albedo. Substituting the function $\psi_b(\tau,-\mu)$ given by Eq. (6.28) into Eq. (6.254), we have

$$\mathcal{W}_\epsilon(\tau_v,\Omega_v)=-\epsilon B(T_s)\int_{\Omega_-} I^*(\tau_0,\Omega;\Omega_v)\mu\,\mathrm{d}\Omega\,. \qquad (6.255)$$

References

1. G. I. Bell, S. Glasstone: *Nuclear reactor theory* (Van Nostrand, New York, Reinholt 1970)
2. M. A. Box, S. A. W. Gerstl, C. Simmer: Application of the adjoint formulation to the calculation of atmospheric radiative effects, *Beitr. Phys. Atmosph.*, **61**, 303–311 (1988)
3. M. Buchwitz, R. de Beek, J. P. Burrows, H. Bowensmann, T. Warneke, J. Notholt, J. F. Meirink, A. P. H. Goede, P. Bergamaschi, S. Koerner, M. Heimann, and A. Schulz: Atmospheric methane and carbon dioxide from SCIAMACHY satellite data: initial comparison with chemistry and transport models, *Atmos. Chem. Phys.*, **5**, 941–962 (2005)
4. S. Chandrasekhar: *Radiative transfer* (Oxford University Press, London, 1950)
5. Fu-Lung Chang and Zhanqing Li: Retrieving vertical profiles of water-cloud droplet effective radius: Algorithm modification and preliminary application, *J. Geophys. Res.*, **108**, D24, 4763, doi:10.1029/2003JD003906, (2003)
6. J. W. Hovenier, C. Van der Mee, H. Domke: *Transfer of polarized light in planetary atmospheres. Basic concepts and practical methods* (Kluwer Academic Publishers, Dordrecht Boston London, 2004)
7. Alexander A. Kokhanovsky: *Cloud optics* (Springer, Netherlands, 2003)
8. A. A. Kokhanovsky: Local optical characteristics of mixed clouds: simple parameterizations, *Atmos. Res.*, in press (2007)
9. G. A. Korn, T. M. Korn: *Mathematical handbook for scientists and engineers* (McGraw-Hill Book Company, New York San Francisco Toronto London Sydney, 1968)
10. V. P. Kozlov: Design of experiments related to the inverse problem of mathematical physics. In: *Mathematical theory of experiment design*, ed. by C. M. Ermakov, pp. 216–246, Nauka, Moscow, 1983, in Russian.
11. K. N. Liou: *An introduction to atmospheric radiation* (Academic Press, New York, 1980)
12. J. Lenoble: *Atmospheric radiative transfer* (A. Deepak Publishing, Hampton, Virginia USA, 1993)
13. Y. L. Luke: *Mathematical functions and their approximations* (Academic Press Inc., New York San Francisco London, 1975)
14. G. I. Marchuk: Equation for the value of information from weather satellites and formulation of inverse problems, *Cosmic Res.*, **(**2), 394–409 (1964)
15. Q. Min, L. E. Harrison: An adjoint formulation of the radiative transfer method, *J. Geophys. Res.*, **101**, D1, 1635–1640 (1996)
16. I. N. Polonsky, M. A. Box: General perturbation technique for the calculation of radiative effects in scattering and absorbing media, *J. Opt. Soc. of America*, **19**, Issue 11, page 2281 (2002)
17. I. N. Polonsky, M. A. Box, A. B. Davis: Radiative transfer through inhomogeneous turbid media: implementation of the adjoint perturbation approach at the first order, *J. Quant. Spectrosc. Radiat. Transfer*, **78**, 85–98 (2003)
18. G. C. Pomraning: *Linear kinetic theory and particle transport in stochastic mixtures* (World Scientific Publishing, Singapore New Jersey London Hong Kong, 1991)
19. C. D. Rodgers: *Inverse methods for atmospheric sounding: theory and practice* (World Scientific, Singapore, 2000)
20. V. V. Rozanov, Yu. M. Timofeev: Retrieval of vertical profiles of atmospheric aerosol optical characteristics using satellite measurements of outgoing radiation

in 0.76 micrometers absorption band, *Izvestiya AN. Physics of Atmosphere and Ocean*, **30**, N6, 779–785 (1994)
21. V. V. Rozanov and A. A. Kokhanovsky: Semi-analytical cloud retrieval algorithm as applied to the cloud top altitude and the cloud geometrical thickness determination from top of atmosphere reflectance measurement in the oxygen absorption bands, *J. Geophys. Res.*, **109**, D05202, 10.1029/2003JD004104, (2004)
22. A. Rozanov, V. Rozanov, M. Buchwitz, A. Kokhanovsky, J. P. Burrows: SCIATRAN 2.0 – A new radiative transfer model for geophysical applications in the 175–2400 nm spectral region, *Adv. Space Res.*, doi:10.1016/j.asr.2005.03.012
23. A. Rozanov, H. Bovensmann, A. Bracher, S. Hrechanyy, V. Rozanov, M. Sinnhuber, F. Stroh, J. P. Burrows: NO_2 and BrO vertical profile retrieval from SCIAMACHY limb measurements: Sensitivity studies, *Adv. Space Res.*, **36**, 846–854 (2005)
24. V. V. Rozanov: Adjoint radiative transfer equation and inverse problems. In: *Light Scattering Reviews*, ed. by A. A. Kokhanovsky. (Springer, Berlin, 2006)
25. V. V. Rozanov, A. V. Rozanov: Generalized form of the direct and adjoint radiative transfer equations. *J. Quant. Spectrosc. Radiat. Transfer*, **104**, 155–170 (2007).
26. A. Rozanov, V. Rozanov, J. P. Burrows: Software package SCIATRAN 2.1 – New developments in the radiative transfer modeling and the retrieval technique. Paper presented at COSPAR 2006, to appear in *Adv. Space Res.*, 2007
27. G. E. Thomas, K. Stamnes: *Radiative transfer in the atmosphere and ocean* (Cambridge University Press, Cambridge, 1999)
28. A. N. Tikhonov, V. Ya. Arsenin: *Solutions of ill-posed problems* (Halsted Press, Washington, DC 1977)
29. Yu. M. Timofeyev, A. V. Vasilyev, V. V. Rozanov: Information content of the spectral measurements of the 0.76 µm O_2 outgoing radiation with respect to the vertical aerosol optical properties, *Adv. Space Res.*, **16**, No. 10, 1091–1094 (1995)
30. E. A. Ustinov: Adjoint sensitivity analysis of radiative transfer equation: temperature and gas mixing ratio weighting functions for remote sensing of scattering atmospheres in thermal IR, *J. Quant. Spectrosc. Radiat. Transfer*, **68**, 195–211 (2001)
31. E. A. Ustinov: Adjoint sensitivity analysis of radiative transfer equation: 2. Applications to retrievals of temperature in scattering atmospheres in thermal IR. *J. Quant. Spectrosc. Radiat. Transfer*, **73**, 29–40 (2002)
32. E.A. Ustinov: Atmospheric weighting functions and surface partial derivatives for remote sensing of scattering planetary atmospheres in thermal spectral region: general adjoint approach, *J. Quant. Spectrosc. Radiat. Transfer*, **92**, 351–371 (2005)
33. V. Volterra: *Theory of functionals and of integral and integro-differential equations* (Dover, New York, 1959)